THESIS FOR THE DEGREE OF DOCTOR OF PHILOSOPHY

Systems biology of yeast metabolism

- Understanding metabolism through proteomics and constraint-based modeling

Carl Malina

Department of Biology and Biological Engineering
CHALMERS UNIVERSITY OF TECHNOLOGY
Gothenburg, Sweden 2021

Systems biology of yeast metabolism
- Understanding metabolism through proteomics and constraint-based modeling

CARL MALINA
ISBN 978-91-7905-520-2

Doktorsavhandlingar vid Chalmers tekniska högskola
Ny serie nr 4987
ISSN 0346-718X

Department of Biology and Biological Engineering
Chalmers University of Technology
SE-412 96 Gothenburg
Sweden
Telephone + 46 (0)31-772 1000

Cover: **The systems biology workflow used for studying metabolism**

Printed by Chalmers Reproservice Gothenburg, Sweden 2021

Systems biology of yeast metabolism

- Understanding metabolism through proteomics and constraint-based modeling

Carl Malina
Department of Biology and Biological Engineering
Chalmers University of Technology

Abstract

Metabolism is the set of all chemical reactions that occur inside of cells. By providing all the building blocks that are required for sustaining a cellular state and cell proliferation, metabolism is at the core of cellular function. Therefore, in order to understand cellular function it is important to understand cellular metabolism. The cellular metabolic network comprises thousands of reactions even in the simplest of organisms. Due to the high complexity, a holistic approach is required to study and understand the interactions between different parts of metabolism giving rise to cellular phenotypes.

In this thesis, a systems biology approach to studying metabolism in yeast, mainly with a focus on *Saccharomyces cerevisiae* (baker's yeast), was used. This approach consisted of combining proteomic analysis with constraint-based modeling to gain insights into different aspects of metabolism. First, the role of mitochondria in cellular metabolism throughout diauxic growth was evaluated, showing that mitochondria balance their role as a biosynthetic hub and center for energy generation depending on the mode of cellular metabolism. Next, the construction of a model of mitochondrial metabolism describing the essential mitochondrial processes of protein import and cofactor metabolism as well as the proton motive force driving the generation of free energy (in the form of ATP) is described and evaluated. The model was used to investigate the dynamics in mitochondrial metabolism and the requirement of these processes.

Second, the constraints on cellular metabolism arising from finite protein resources was investigated in two studies. The first study evaluated the effect of amino acid supplementation on the physiology and allocation of protein resources. This study showed that as the burden of producing amino acids is relieved, the cells can allocate more protein to the translation, which allows the cells to grow faster. In the second study, a quantitative comparison of four yeast species was performed to evaluate the underlying causes of overflow metabolism, which is the seemingly wasteful strategy of using aerobic fermentation instead of the more efficient respiratory pathway for glucose utilization. We showed that overflow metabolism in yeast is linked to adaptations in metabolism and protein translation. This phenomenon is seen in cells ranging from bacteria to yeast and cancer cells, and the insights provided in our study could therefore be valuable in understanding the metabolism not only in yeast but in more complex systems.

Keywords: *Systems biology, yeast, metabolism, proteomics, constraint-based modeling*

Systembiologi av metabolismen i jäst
- Undersökning av metabolismen genom proteomik och villkorsbaserad modellering

Carl Malina
Institutionen för Biologi och Bioteknik
Chalmers Tekniska Högskola

Sammanfattning

Metabolism är samlingen av alla kemiska reaktioner som äger rum i celler. Genom att förse cellen med de byggstenar som behövs för att upprätthålla ett cellulärt tillstånd samt tillväxt av cellen är metabolismen en central cellulär funktion. För att förstå hur celler fungerar är det därför viktigt att förstå metabolismen. Det metaboliska nätverket i celler innefattar tusentals reaktioner, även i de allra simplaste av organismer. Givet den höga komplexiteten behövs ett holistiskt tillvägagångssätt för att förstå hur olika delar av metabolismen är kopplade till olika cellulära fenotyper.

I denna avhandling användes ett systembiologiskt tillvägagångssätt för att studera metabolismen i jäst, med ett fokus på *Saccharomyces cerevisiae* (bagerijäst). Detta innefattade en kombination av proteomikanalys och simuleringar med villkorsbaserade modeller med syfte att ge en inblick i olika aspekter av metabolismen. Först utvärderades rollen av mitokondrier under de tillväxtfaser som inträffar vid odling av jäst, vilket visade att mitokondrier balanserar sin roll som biosyntetiska hubbar och center för generering av energi beroende på cellens metaboliska tillstånd. Därefter beskrivs konstruerandet och utvärderingen av en modell över mitokondrien, innefattande en beskrivning av mitokondriell proteinimport, syntes av cofaktorer samt den protontranslokerande kraft som driver genereringen av fri energi (i form av ATP). Modellen användes till att studera dynamiken i den mitokondriella metabolismen samt behovet av ovanstående processer.

Sedan utvärderades de restriktioner som verkar på den cellulära metabolismen, med ursprung i cellens begränsade proteinresurser, i två studier. Den första studien utvärderade effekten av att tillsätta aminosyror på fysiologin och allokeringen av proteinresurser. Studien visade att när bördan som utgörs av att syntetisera aminosyror minskas, kan cellen omfördela protein till tillverkningen av nya protein, vilket leder till att cellen kan växa snabbare. I den andra studien utfördes en kvantitativ jämförelse mellan fyra jästarter för att utvärdera de underliggande orsakerna till att celler använder en till synes slösaktig aerob fermentering istället för den mer effektiva respirationen för att bryta ner glukos. Vi påvisade att denna metaboliska strategi är kopplad till adapteringar i metabolismen och proteinsyntesen. Existensen av detta fenomen sträcker sig från bakterier till jäst och cancerceller, och insikterna från denna studie kan därför appliceras inte bara i jäst utan även i mer komplexa system.

Nyckelord: *Systembiologi, jäst, metabolism, proteomik, villkorsbaserad modellering*

List of publications

This thesis is based on the following publications and manuscript

Paper I: **Carl Malina**, Christer Larsson, Jens Nielsen. Yeast mitochondria: an overview of mitochondrial biology and the potential of mitochondrial systems biology. *FEMS Yeast Res.* **18**(5), foy40 (2018).

Paper II: Francesca Di Bartolomeo*, **Carl Malina***, Kate Campbell, Maurizio Mormino, Johannes Fuchs, Egor Vorontsov, Claes M Gustafsson, Jens Nielsen. Absolute yeast mitochondrial proteome quantification reveals trade-off between biosynthesis and energy generation during diauxic shift. *Proc Natl Acad Sci USA* **117**(13), 7524-7535 (2020).

Paper III: **Carl Malina**, Francesca Di Bartolomeo, Eduard J Kerkhoven, Jens Nielsen. Constraint-based modeling of yeast mitochondria reveals the dynamics of protein import and iron-sulfur cluster biosynthesis. *Manuscript under revision.*

Paper IV: Johan Björkeroth, Kate Campbell, **Carl Malina**, Rosemary Yu, Francesca Di Bartolomeo, Jens Nielsen. Proteome reallocation from amino acid biosynthesis to ribosomes enables yeast to grow faster in rich media. *Proc Natl Acad Sci USA* **117**(35), 21804-21812 (2020).

Paper V: **Carl Malina**, Rosemary Yu, Johan Björkeroth, Eduard J Kerkhoven, Jens Nielsen. Adaptations in metabolism and protein translation give rise to the Crabtree effect in yeast. *Submitted manuscript.*

*contributed equally

Contribution summary

Paper I. Performed the literature review, wrote the original manuscript and constructed the figures.

Paper II. Co-designed the study, performed experiments, data analysis and wrote parts of the original manuscript.

Paper III. Co-designed the study, constructed the model, performed simulations, analyzed results and wrote the original manuscript.

Paper IV. Performed some of the experiments, contributed to data analysis and manuscript preparation.

Paper V. Co-designed the study, performed experiments and simulations, analyzed data and wrote the original manuscript.

Preface

This dissertation serves as partial fulfilment of the requirements to obtain the degree of Doctor of Philosophy at the Department of Biology and Biological Engineering at Chalmers University of Technology. The PhD research was carried out between October 2016 and September 2021 at the division of Systems and Synthetic Biology under the supervision of Jens Nielsen. The project was co-supervised by Christer Larsson and Eduard Kerkhoven and examined by Ivan Mijakovic. The project was funded by the Knut and Alice Wallenberg Foundation.

Carl Malina
September 2021

Contents

Abbreviations

1,3bPG	1,3-bisphosphoglycerate
2PG	2-phosphoglycerate
3PG	3-phosphoglycerate
6PG	6-phosphogluconate
6PGL	6-phosphogluconolactone
ATP	Adenosine triphosphate
ACP	Acyl-carrier protein
BCAA	Branched-chain amino acids
CL	Cardiolipin
DHAP	Dihydroxyacetone phosphate
E4P	Erythrose-4-phosphate
ETC	Electron transport chain
F6P	Fructose-6-phosphate
F1,6bP	Fructose-1,6-bisphosphate
FAS	Fatty acid synthesis
Fe-S clusters	iron-sulfur clusters
G6P	Glucose-6-phosphate
GA3P	Glyceraldehyde-3-phosphate
GCV	Glycine cleavage system
IDH	Isocitrate dehydrogenase
KGD	α-ketoglutarate dehydrogenase
MLCL	Monolysocardiolipin
MPC	Mitochondrial pyruvate carrier
NADH	Nicotineamide adenine dinucleotide
NADPH	Nicotineamide adenine dinucleotide phosphate
PCA	Pricipal component analysis
PDH	Pyruvate dehydrogenase
PE	Phosphatidylethanolamine
PEP	Phosphoenolpyruvate
PMF	Proton motive force
PPP	Pentose phosphate pathway
PS	Phosphatidylserine
Ru5P	Ribulose-5-phosphate
R5P	Ribose-5-phosphate
RQ	respiratory quotient
SDH	Succinate dehydrogenase
SGD	Saccharomyces genome database
TCA	Tricarboxylic acid
WGD	Whole-genome duplication

What I cannot create, I do not understand
-Richard Feynman

Background

Biology is the study of life and "what is life?", as posed by Schrödinger [1], has been a fundamental question for biologists to tackle. The fundamental unit of life is the cell. Within cells, the genetic material encoding all the components required for cell proliferation is stored in the genome. The flow of genetic information in cells is described by the central dogma of molecular biology. In its modern interpretation, it describes the transcription of DNA into RNA and the translation of RNA into protein **Figure 1A**. Proteins are diverse in their functions, ranging from structural proteins to transporters and metabolic enzymes, which catalyze the reactions converting nutrients into cellular building blocks. For a cell to function, the above mentioned processes need to be precisely regulated and organized. Following the genomics revolution and the development of high-throughput technologies for studying biological macromolecules, we are now able to study the entire set of genes (genome), transcripts (transcriptome), proteins (proteome) and metabolites (metabolome) as illustrated in **Figure 1B**, allowing the generation of large amounts of biological data [2]. To understand the behavior of cells, there is a need for understanding the complex interactions between these different layers, requiring a shift from studying individual constituents to studying living organism as a system of its components and their interactions.

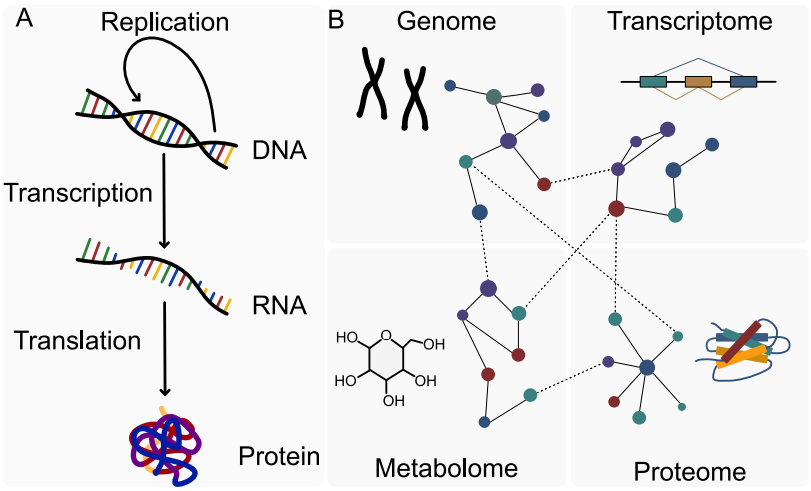

Figure 1 The central dogma of biology in the omics era. (A) The central dogma of molecular biology describing the flow of information from DNA to RNA to protein. (B) The development of high-throughput techniques has led to an evolution of new ways to study the central dogma. Current techniques for omics analysis not only allow for studying the entirety of molecules involved in each layer but also for studying the interaction between layers.

1.1 Systems biology

Systems biology is an interdisciplinary field that lies at the intersection of biology, engineering, mathematics and computer science. It emerged to meet the growing need of a systematic framework for analyzing and integrating the increasing amount of biological data being generated in the post-genomics era [3–5]. The field aims to build, quantify, and understand the complex networks that form living organisms using a holistic approach comprised of a combination of computational and mathematical models with large scale experimental data. There is in principle two complementary approaches in systems biology [6]. Top-down systems biology involves the integrative analysis of omics data to gain insight into the cellular functions [7]. In many cases, there is not a specific hypothesis when using a top-down approach, but often hypotheses are generated and tested against the data as the analysis proceeds, making top-down systems biology an inductive scientific approach [8]. Typical top-down systems biology approaches involve iterative cycles starting with the generation of large datasets, such as proteomics and/or transcriptomic data, that are analyzed to find correlations between the components of the system [6]. The cycle ends with the generation of hypotheses that can predict new correlation, which can be further evaluated in a new round of experiments. Top-down systems biology studies often rely on the use of different models at various stages of the analysis. The models used in top-down systems biology are phenomenological, meaning that they rely more on data and require less mechanistic knowledge than those used in bottom-up approaches [6]. As such, top-down systems biology is useful in mapping cellular functions at the genome-scale, identifying previously uncharacterized interactions between the components of the system, and for generating hypotheses that can drive future studies. Bottom-up systems biology involves the formulation of mechanistic models for specific processes or pathways based on a detailed description of its constituents and the idea that system behavior emerges from the interactions of these constituents, as exemplified by a kinetic model of yeast glycolysis [9]. The ultimate goal of bottom-up systems biology is to combine these individual models into a holistic model describing the function of the system as a whole [6]. A main challenge in the construction of models in bottom-up systems biology is the requirement of high-quality data on the properties of the system components, such as kinetic and physiochemical properties of enzymes, which to a large extent depends on *in vitro* studies of individual enzymes and, when such data is unavailable, on parameter estimation.

The common feature of the two approaches is that they can both be used to elucidate the interplay between the components of the system that underlie the emergent properties that give rise to the cellular functions of a biological system, which is not possible using a reductionist molecular biology approach [7]. In the work included in this thesis, I made use of both the top-down and bottom-up approaches to gain insight into different aspects of cellular phenotypes and overall physiology. This includes using proteomic- and lipidomic data to study the role of mitochondria in cellular function during the course of a batch cultivation (**Paper II**). In **Paper III**, I used a bottom-up approach involving the reconstruction of a model of the two essential processes of mitochondrial protein import and iron-sulfur cluster

biogenesis, that I then used to investigate the energetics and dynamics of the processes. Finally, an approach combining integrative analysis of proteomic data and model simulations was used to understand the behavioral changes of yeast grown in rich and minimal media (**Paper IV**) as well as to investigate the underlying mechanisms of the Crabtree effect by comparing four different yeasts (**Paper V**).

1.2 *Saccharomyces cerevisiae* (and some of its relatives)

Saccharomyces cerevisae, commonly known as baker's yeast, has been employed by humans for baking and brewing for thousands of years. The close connection to human activities was a contributing factor to the extensive research on yeast genetics and physiology that has been ongoing for the last century and a half, making *S. cerevisiae* perhaps the most well-studied eukaryal organism. It is widely used as a model organism for studying eukaryal cell physiology and molecular events, including human disease [10]. The importance of the yeast as a model organism is further highlighted by the fact that it was the first organism for which a complete chromosome was sequenced [11] and the first eukaryal organism with a complete genome sequence available [12]. There are several factors that make the yeast an attractive model organism. First, *S. cerevisiae* is a unicellular fast-growing microorganism that can easily be cultivated in a simple and inexpensive media, allowing the cultivation under controlled conditions that allow for a high reproducibility. Second, there is a large and well-curated research infrastructure available, such as the Saccharomyces Genome Database (SGD) [13]. Third, a large number of high-throughput technologies are available which has resulted in the generation of a vast amount of biological data, including transcriptomic, proteomic and metabolomic data. Furthermore, although yeast is a relatively simple organism, many cellular processes are conserved in higher eukaryal organisms, and a large fraction of *S. cerevisiae* genes have human orthologues. Lastly, yeast is amenable to genetic manipulation enabling the deletion, insertion, or manipulation of any sequence in its genome and a complete single gene deletion collection is available [14]. The relative ease by which the *S. cerevisiae* genome can be manipulated has contributed to the extensive use of the yeast as a cell factory for producing pharmaceuticals, chemicals and biofuels [15, 16].

While much attention has been focused on *S. cerevisiae*, other yeasts have also come to play important roles in research and biotechnological applications. Since most of the work carried out in this thesis was performed using *S. cerevisiae*, unless otherwise stated yeast will be referring to this species and the other three yeasts used, namely *Schizosaccharomyces pombe*, *Kluyveromyces marxianus* and *Scheffersomyces stipitis*, will only be described briefly here. *S. pombe* is a fission yeast that diverged from the *S. cerevisiae* lineage more than 300 million years ago. Like baker's yeast, it was one of the early eukaryal organisms to have its complete genome sequenced [17]. Being a fission yeast, its cell division more closely resembles that of human cells than does *S. cerevisiae*'s, it is another commonly used model organism for studying eukaryal cells, especially for studies on the genetics of the cell cycle [18]. Although different in many aspects, the metabolism of the two yeasts, which is the main focus of this thesis, is very similar and they both experience aerobic fermentation. *K. marxianus* is a

dairy yeast that has emerged as an attractive alternative for industrial applications due to a number of favorable characteristics [19]. It has a high thermotolerance, a very high maximum specific growth rate and can assimilate sugars, such as xylose and lactose, which *S. cerevisiae* is unable to utilize. *K. marxianus* is Crabtree-negative but does exhibit respiro-fermentative growth in response to limitations in oxygen availability. Finally, *S. stipitis*, like *K. marxianus*, is Crabtree-negative and only ferments under conditions of limited oxygen availability. The yeast is most known for its ability to efficiently utilize pentose sugars [20]. The specifics of overflow metabolism and the Crabtree effect will be discussed in section 1.3.

1.3 Metabolism

Every organism relies on the ability to take up and utilize nutrients from its surroundings to generate energy and building blocks required for cell growth. Metabolism consists of thousands of reactions interconverting chemical compounds, referred to as metabolites, some of which are biomass precursors and some that are secreted as by-products. Metabolic reactions are commonly grouped into metabolic pathways containing series of linked reactions. Although some reactions can occur spontaneously, most reactions require the catalysis by enzymes, a specific class of proteins dedicated to accelerating the rate of reactions to proceed at rates high enough to sustain growth. A simplified overview of metabolism is illustrated in **Figure 2**.

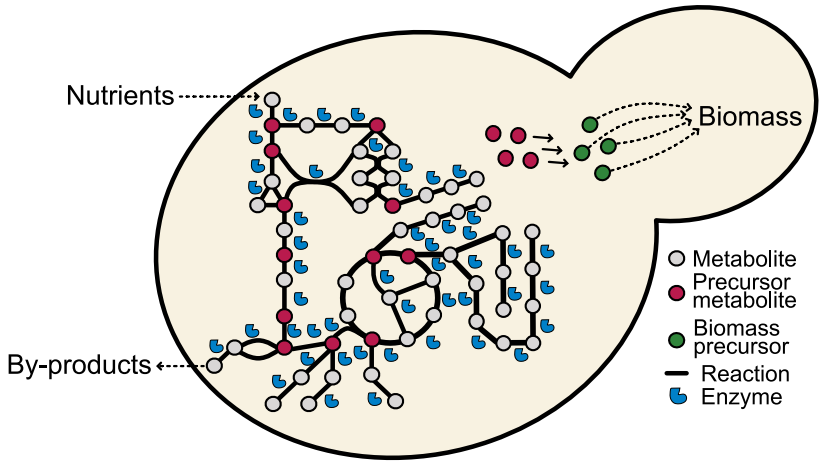

Figure 2 A simplified representation of a metabolic network.

Metabolism is broadly categorized into the opposing processes of catabolism and anabolism [7]. Catabolism involves all reactions responsible for breaking down carbon- and energy sources into 12 precursor metabolites that are used in anabolic reactions to synthesize all building blocks that are used to synthesize biomass precursors. These building blocks include nucleotides, amino acids, monosacccharides and fatty acids that are polymerized into the main constituents of biomass: DNA, RNA, proteins, carbohydrates and lipids. Catabolism further involves the generation of free energy stored mainly in the form of adenosine triphosphate (ATP), the main energy currency of the cell, as well as redox power stored in nicotineamide adenine dinucleotide phosphate (NADPH) or nicotineamide adenine dinucleotide (NADH). NADPH is mainly used in the biosynthesis of macromolecules. NADH is either re-oxidized by

the conversion of precursor metabolites into by-products that are secreted from the cell or in the respiratory chain resulting in the production of ATP through oxidative phosphorylation.

1.3.1 Central carbon and energy metabolism

Central carbon metabolism is the series of metabolic reactions required for the synthesis of precursor metabolites, that form the basis of biomass, as well as the generation of energy and redox power required for biomass production. It can be broadly divided into glycolysis, the pentose phosphate pathway (PPP), the tricarboxylic acid (TCA) cycle and oxidative phosphorylation. As an understanding of central carbon metabolism is important for the research performed in this thesis, I will give a brief overview of the different pathways involved.

Glycolysis

Glycolysis is the set of reactions converting glucose, which is the preferred carbon source for *S. cerevisiae* and many other organisms, into pyruvate [21]. It should be noted that other sugars, such as fructose, can also enter glycolysis but for the purpose of the work in this thesis, only glycolysis starting from glucose will be considered. Glycolysis can be divided into two phases. The first phase, often referred to as the preparatory phase, involves the investment of energy in the form of 2 molecules of ATP to convert glucose into two molecules of the three-carbon sugar-phosphate glyceraldehyde-3-phosphate (GA3P). The first ATP is invested in the phosphorylation of glucose to form glucose-6-phosphate (G6P), which is catalyzed by either the hexokinases Hxk1 and Hxk2 or glucokinase Glk1. G6P is then further isomerized to form fructose-6-phosphate (F6P), catalyzed by phosphoglucose isomerase Pgi1. In the following step, a molecule of ATP is invested in the phosphorylation of F6P to form fructose-1,6-bisphosphate (F1,6bP), catalyzed by phosphofructokinases Pfk1 and Pfk2. Fructose bisphosphate aldolase Fba1 then splits F1,6bP into GA3P and dihydroxyacetone phosphate (DHAP), which can be converted to GA3P by triose phosphate isomerase Tpi1. The second stage of glycolysis, called the energy generation phase, starts with the conversion of GA3P to 1,3-bisphosphoglycerate (1,3bPG) by glyceraldehyde-3-phosphate dehydrogenase Tdh1, Thd2 or Tdh3, resulting in the generation of NADH. 1,3bPG is then converted into 3-phosphoglycerate (3PG) by phosphoglycerate kinase Pgk1, generating one molecule of ATP. In the following two steps, 3PG in converted into 2-phosphoglycerate (2PG), which is in turn converted into phosphoenolpyruvate (PEP), catalyzed by phosphoglycerate mutase Gpm1 and phosphopyruvate hydratase Eno1 or Eno2, respectively. Finally, PEP is converted into pyruvate by pyruvate kinase Cdc19 (Pyk1) or Pyk2, resulting in the synthesis of one ATP. Overall, glycolysis results in the generation of two molecules of NADH and 2 molecules of ATP per molecule of glucose.

Pentose phosphate pathway

The PPP generates reducing power in the form of NADPH, as well as precursors for nucleotide and amino acid synthesis. In the PPP, G6P is converted to 6-phosphogluconolactone (6PGL), catalyzed by G6P dehydrogenase Zwf1. 6PGL is converted into 6-phosphogluconate (6PG) by 6-phosphogluconolactonase Sol3 or Sol4, and 6PG is in turn converted to ribulose-5-

phosphate (Ru5P) and carbon dioxide by 6-phosphogluconate dehydrogenase Gnd1 or Gnd2. This initial part of the PPP is referred to as the oxidative branch and results in the generation of 2 molecules of NADPH per molecule of G6P. The Ru5P generated is converted via Rki1, Rpe1, Tkl1, Tkl2, Tal1 and Nqm1 into the glycolytic intermediates GA3P and F6P or into ribose-5-phosphate (R5P) or erythrose-4-phosphate (E4P), that serve as precursors for the synthesis of for example aromatic amino acids and nucleotides.

TCA cycle

The TCA cycle is a series of reactions responsible for complete oxidation of acetyl-CoA to release energy and redox power. During respiratory metabolism, it is the main pathway for pyruvate utilization. In eukaryal cells, the TCA cycle takes place in the mitochondrial matrix. Pyruvate produced in glycolysis is transported into mitochondria via the mitochondrial pyruvate carrier (MPC). It is then converted into acetyl-CoA by the pyruvate dehydrogenase (PDH) complex, consisting of subunits Pda1, Pdb1, Pdx1, Lpd1 and Lat1, resulting in the formation of NADH and CO_2. In the next couple of reactions, acetyl-CoA is combined with oxaloacetate by citrate synthase Cit1, to form citrate, which is converted into isocitrate by aconitase Aco1. In the next step, isocitrate is converted into α-ketoglutarate by isocitrate dehydrogenase (IDH), consisting of subunits Idh1 and Idh2, resulting in the formation of NADH and CO_2. This step can also be carried out by NADP-dependent isocitrate dehydrogenase Idp1. α-ketoglutarate dehydrogenase (KGD), consisting of Kgd1 and Kgd2, convert α-ketoglutarate into succinyl-CoA, forming an additional NADH and CO_2. Succinyl-CoA is converted into succinate by succinyl-CoA ligase, Lsc1 and Lsc2, generating an ATP, and succinate is further converted into fumarate by the succinate dehydrogenase complex (SDH), resulting in the reduction of the redox carrier FAD to $FADH_2$. Finally, fumarate is converted into malate by fumarase Fum1, and malate is converted into oxaloacetate by malate dehydrogenase, forming an NADH, and then the cycle repeats. Overall, the PDH reaction and the TCA cycle generates 4 molecules of NADH, 1 molecule of $FADH_2$, 1 molecule of ATP, as well as 3 molecules of CO_2 per molecule of pyruvate.

Oxidative phosphorylation

In order for the TCA cycle to continue, the reduced redox factors, NADH and $FADH_2$ must be re-oxidized. In yeast, under aerobic conditions, the electrons from these cofactors are transferred to molecular oxygen through a series of electron acceptors, organized as protein complexes in the mitochondrial inner membrane. Electrons enter the electron transport chain (ETC) either through the oxidation of NADH at NADH dehydrogenase or at SDH where $FADH_2$ is re-oxidized to FAD. In some yeasts, including *S. cerevisiae*, complex I is missing and NADH oxidation is instead carried out by internal NADH dehydrogenase Ndi1, for mitochondrial matrix generated NADH, or external dehydrogenases Nde1 and Nde2 facing the intermembrane space for NADH produced in the cytosol. The electrons released are transferred to the electron carrier coenzyme Q. From there, electrons are transferred to ubiquinol-cytochrome c reductase complex (complex III), which reduces cytochrome c. Finally, electrons are transferred from cytochrome c to molecular oxygen through the cytochrome c

oxidase complex (complex IV) resulting in the formation of water. As electrons are transferred, free energy is released, which is used to translocate protons across the inner membrane at complexes III and IV. This results in the generation of a proton motive force (PMF) consisting of a proton gradient and a membrane potential. The gradient is harvested by ATP synthase, that allows protons to re-enter the matrix, resulting in the release of energy which is captured by the formation of ATP.

1.3.2 Overflow metabolism

Cellular resources are finite and the cell needs to optimize its allocation of resources in any given condition. Biological processes depend on enzymes and other proteins to function. As the protein content of the cell is limited, the cell must balance the allocation between the different functions to ensure optimal cellular function. The optimal allocation is dictated by the specific growth conditions and achieved through a finely tuned regulation of transcription and translation as well as the activity of individual enzymes [22–24]. The finite proteome resources result in a trade-off in allocation between different sectors of the proteome. An example of such a trade-off is the allocation between ribosomes and metabolic proteins. It has been shown that the requirement of ribosomes scales linearly with the growth rate [25], giving rise to a trade-off between different metabolic strategies used.

Overflow metabolism is the result of a trade-off between the rate and yield of ATP production. It is signified by a shift from respiratory to fermentative metabolism even at fully aerobic conditions [26]. This results in an increased substrate, for example glucose, consumption rate and an increased channeling of carbon flux through fermentation, ultimately resulting in the secretion of fermentation by-products and thus a lower yield of ATP production (**Figure 3**).

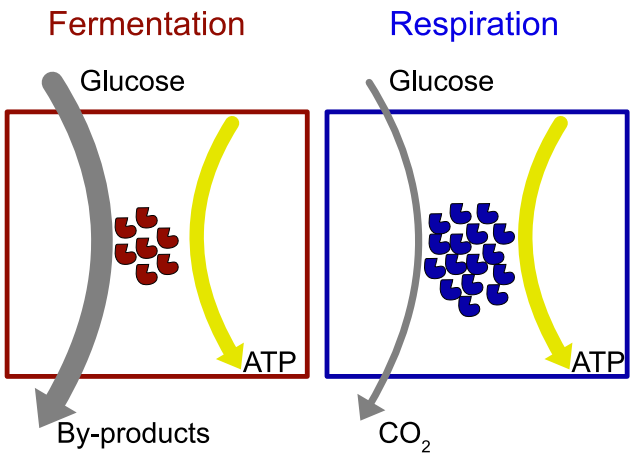

Figure 3 Comparison of the fermentative and respiratory pathways for energy generation. Fermentation and respiration differ in the glucose flux and proteome mass required to produce an equivalent amount of ATP. Fermentation is less efficient in terms of ATP produced per glucose and therefore requires a high glucose flux. Respiration is more efficient in terms of ATP yield per substrate, but is less efficient in terms of the yield per protein mass required.

In many organisms, glucose is the preferred substrate. Respiratory consumption of glucose, which in addition to glycolysis involves the full oxidation of pyruvate to carbon dioxide and water through the concerted action of the TCA cycle, the ETC and ATP synthase, is the

most efficient pathway in terms of the amount of ATP generated per molecule of substrate. However, apart from the glycolytic proteins, the pathway requires the synthesis of a large number of mitochondrial proteins involved in oxidative phosphorylation while the fermentative pathway only requires the synthesis of a few additional cytosolic enzymes. Fermentation thus has a higher catalytic rate than respiration, resulting in more ATP synthesized per enzyme mass. Overflow metabolism is therefore a favorable strategy when fast ATP production is required.

In yeast, overflow metabolism is referred to as the Crabtree effect [27, 28] and it results in the secretion of high levels of ethanol, and to a smaller extent acetate. Not all yeasts experience the Crabtree effect, and yeasts are commonly classified as Crabtree-positive or negative based the presence or absence of the Crabtree effect. Some yeasts, such as *K. marxianus* and *S. stipitis* do not experience the Crabtree effect, while still growing at similar rates as Crabtree-positive yeasts. The underlying causes of the Crabtree effect will be evaluated in part II of this thesis.

1.4 Mitochondria

The first part of this thesis is focused on studying mitochondria and their role in the overall function of the cells. In this section, I will go through **Paper I** and give an overview of mitochondrial biology, including mitochondrial evolution, the general characteristic of the organelle as well as the role of mitochondria in various metabolic pathways.

1.4.1 Mitochondrial evolution

Mitochondria are organelles that are present in the vast majority of all eukaryal cells. The organelle resulted from an endosymbiotic event where an α-proteobacterium was taken up by a host cell [29]. The nature of the host has been debated and it was originally thought that the host was a primitive eukaryon with an anaerobic lifestyle, lacking many of the modern features of eukaryal cells, that engulfed the mitochondrial progenitor through phagocytosis [30]. However, more recent studies point towards the host being an archeabacterium, and that the complexity of eukaryal cells evolved after acquiring the mitochondrial ancestor [31]. It has been hypothesized that a reductive evolution of the endosymbiont and specialization into mitochondria resulted in expansion of the bioenergetic membrane surface area [32]. Ultimately, this would result in an increase in the energy per gene allowing for a large expansion of the number of genes expressed, supporting the evolution of the complex traits that are hallmarks of eukaryal cells. As a result of the reductive evolution, the majority of all mitochondrial genes were either lost or transferred to the nuclear genome. Modern mitochondrial genomes only encode a small number of proteins, that are translated on mitochondrial ribosomes. In the case of *S. cerevisiae*, the mitochondrial genome encodes eight proteins of which seven are core subunits of the respiratory chain and one is a ribosomal protein of the small subunit of the mitochondrial ribosome.

1.4.2 Mitochondrial structure

Mitochondria are highly dynamic and their morphology is tightly linked to the physiological state, including the bioenergetic requirements, of the cell [33]. The shape, number and size of mitochondria is governed by the opposing forces of fission and fusion, and exponentially growing yeast cells can experience up to two and a half fusion and fission event per minute and cell. Under conditions where the respiratory activity is high, fusion is favored as it generates large and interconnected tubular networks, that allow for efficient mixing of the mitochondrial content, including mitochondrial DNA, proteins and metabolites. When the respiratory activity is low, on the other hand, mitochondrial fission drives the generation of a smaller and fragmented mitochondrial network as illustrated in **Figure 4**.

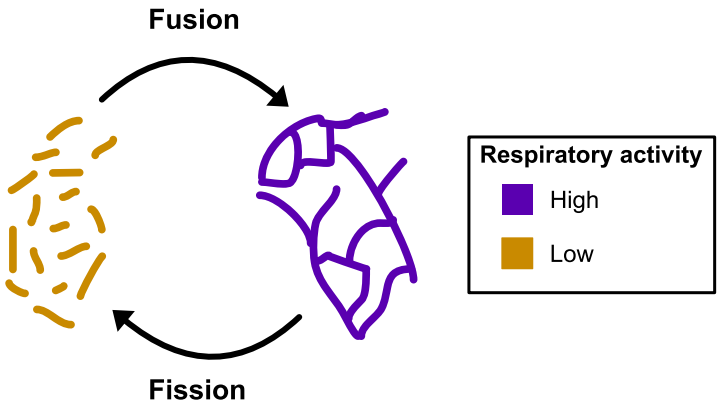

Figure 4 Overview of mitochondrial morphology adaptation to respiratory activity. The mitochondrial morphology is governed by cycles of fission and fusion in response to the respiratory activity. Fragmented mitochondria are preferred when the respiratory activity is low while a fused network is preferred when the respiratory activity is high.

Mitochondria consist of two membranes, the inner- and outer mitochondrial membrane that enclose two aqueous compartments, the intermembrane space (IMS) and the mitochondrial matrix. The structure of mitochondria plays an important role in the function of the organelle. The outer membrane contains porins allowing diffusion of molecules up to 4-5 kDa in size, while the inner membrane is largely impermeable, and therefore only allows the diffusion of small uncharged molecules such as oxygen and carbon dioxide [34]. This creates a compartmentalization, that is crucial for the generation of a proton motive force (PMF), through the pumping of protons from the matrix to the IMS across the mitochondrial inner membrane by the ETC complexes. This force is harnessed by ATP synthase to drive ATP production. However, the compartmentalization also presents a physical barrier for metabolites and to the roughly 99% of the mitochondrial proteins that are synthesized on cytosolic ribosomes and must be imported into the organelle upon synthesis. Consequently, mitochondria rely on a set of carrier proteins for exchanging metabolites with the cytosol [34], as well as a dedicated machinery for protein import. Mitochondrial protein import and its implications will be discussed further in **Paper III**.

1.4.3 Mitochondrial metabolism

Mitochondria have long been known as the powerhouses of eukaryal cells due to their role in cellular energy generation, through the ETC and oxidative phosphorylation, but mitochondria also play an important role in various other metabolic processes. Being the site of the TCA cycle, mitochondria are crucial for the generation of metabolic precursors for biosynthetic pathways. Examples of such pathways are in the synthesis of amino acids. Apart from producing α-ketoglutarate, which is an important precursor for many amino acids, mitochondria are also directly involved in the synthesis of some amino acids. In yeast, mitochondria host the majority of the enzymes involved in the biosynthesis of branched-chain amino acids (BCAA), as well as parts of the pathways for synthesis of arginine and lysine [35].

In addition to the role in amino acid biosynthesis, mitochondria are also involved in synthesis of heme, in which the first and last two steps are localized to mitochondria, as well as iron-sulfur (Fe-S) clusters. Fe-S cluster biosynthesis is one of the essential functions of mitochondria. Fe-S clusters are versatile inorganic cofactors that are found in proteins involved in processes ranging from energy metabolism, biosynthesis, maintenance of DNA, gene expression, and translation [36]. An overview of mitochondrial Fe-S cluster biosynthesis is given in **Figure 5**. Briefly, a [2Fe-2S] cluster is first synthesized on a scaffold protein, Isu1/Isu2, involving the cysteine desulfurase complex consisting of Nfs1, Isd11 and Acp1, as well as Yfh1 and the electron transport chain constituted by NADPH, Yah1 and Arh1. Next, the [2Fe-2S] cluster is transferred to the Grx5 transfer protein, a process catalyzed by the hydrolysis of ATP by Hsp70 protein Ssq1, requiring Jac1 and nucleotide exchange factor Mge1. After transfer to Grx5, the cluster is either inserted into target proteins or further transferred to the machinery responsible for assembly of [4Fe-4S] clusters, consisting of Isa1, Isa2 and Iba57, after which the [4Fe-4S] cluster is inserted into target proteins.

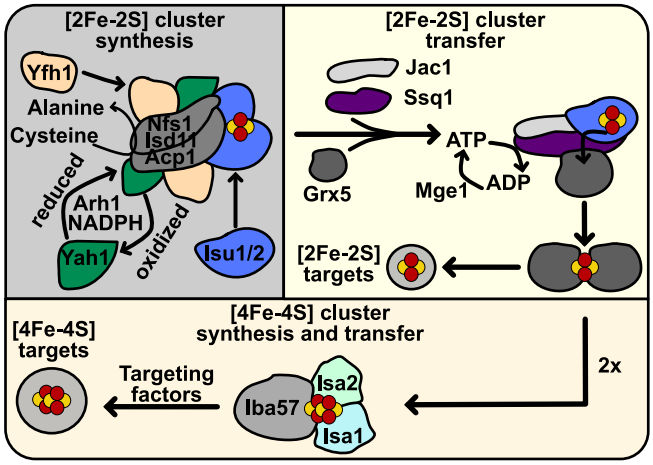

Figure 5 Overview of mitochondrial iron-sulfur cluster biosynthesis in yeast. Briefly, a [2Fe-2S] cluster is first synthesized on a scaffold protein requiring the action of Yfh1, the cysteine desulfurase complex consisting of Nfs1, Isd11 and Acp1, as well as the electron transport chain consisting of Yah1, Arh1 and NADPH. Next, the cluster is transferred to the Grx5 transfer protein dimer through the action of Ssq1, Jac1 and Mge1 requiring the hydrolysis of ATP. From Grx5, the cluster is inserted into target proteins, or transferred to the machinery responsible for synthesis of a [4Fe-4S], consisting of Isa1, Isa2 and Iba57.

Furthermore, mitochondria are involved in phospholipid metabolism, more specifically in the conversion of phosphatidylserine (PS) to phosphatidylethanolamine (PE), as well as

in the synthesis of the mitochondrion-specific phospholipid cardiolipin (CL) [37]. CL is a phospholipid consisting of four acyl chains attached to a dimeric glycerophosphate backbone. This results in a conical shape, that makes the lipid suitable for membranes where curvature is needed. Therefore, the lipid has been found to be enriched in in the cristae of the IMM, where it facilitates the assembly and stabilization of respiratory chain complexes [38]. Mitochondria also contain a machinery for fatty acid synthesis (FAS), which synthesizes fatty acids in an acyl-carrier protein (ACP)-dependent manner resembling bacterial type II FAS [39]. The main role identified for mitochondrial FAS is the synthesis of octanoyl-ACP, which is a precursor of lipoic acid that is an essential cofactor for pyruvate dehydrogenase (PDH), α-ketoglutarate dehydrogenase (KGD) and the glycine cleavage system (GCV).

1.5 Constraint-based modeling of metabolism

Given the complexity of metabolic networks, mathematical models have played an important role in understanding metabolism at a systems level. The types of models used for studying metabolism can be mainly classified as kinetic or stoichiometric. In kinetic models, reaction fluxes and metabolite concentrations are modeled as a function of time using ordinary differential equations [40]. In this thesis, stoichiometric models are employed. Stoichiometric models, often referred to as constraint-based models, infer the reaction fluxes by imposing steady state mass balances around each metabolite of the network [41]. Genome-scale metabolic models (GEMs) comprise a mathematical description of the metabolic network. They contain stoichiometric information on the entire set of known metabolic reactions of an organism, and links them to the corresponding enzymes. As such, GEMs connect genes, reactions and metabolites into a network (**Figure 6A**), which can be represented as a stoichiometric matrix (**Figure 6B**).

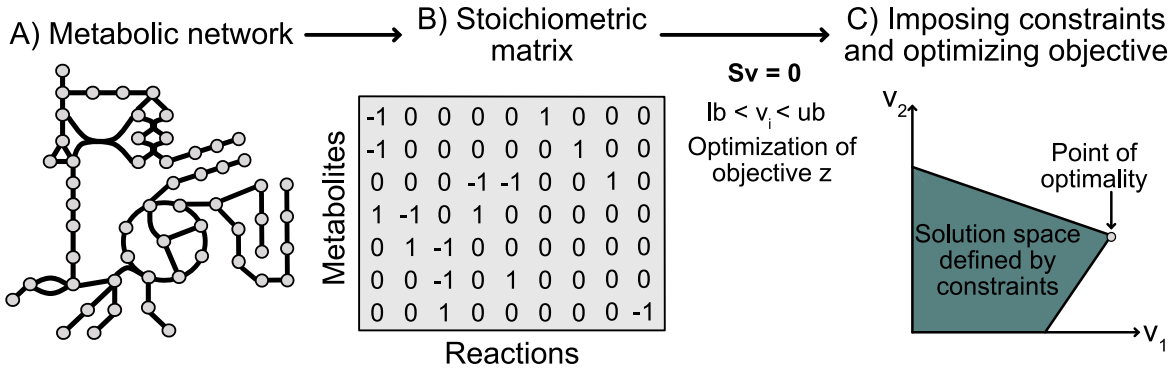

Figure 6 Overview of constraint-based modeling of metabolism. The metabolic network (A) is reconstructed and represented in a stoichiometric matrix (B). The constraints imposed by the stoichiometric matrix are combined with a steady-state assumption and additional constraints on reaction bounds. An objective for optimization is set and simulations are performed to solve the linear set of equations defined to find an optimal solution (C).

Flux balance analysis is a widely used method for analyzing GEMs [42]. A flux balance results from constraints imposed by the stoichiometric matrix implying that the production of any compound must equal the net consumption of the compound at steady state (**Figure 6C**). Additional constraints are imposed by defining the upper and lower bounds of reactions, such as the maximum allowed carbon source uptake rate. These constraints are commonly

inferred from experimental data. Furthermore, an objective such as maximizing cellular growth is used, which together with the mathematical representation defines a system of linear equations. In FBA, these equations are solved using linear programming, which results in the prediction of a flux distribution that optimizes the objective.

During the last decade, an increasing focus in constraint-based modeling has been on developing models that combine FBA with proteome allocation by accounting for enzymatic constraints. A recent framework for accounting for enzyme-constraints in GEMs was developed by Sánchez et al., in 2017 [43]. In this framework, enzymatic constraints are accounted for by incorporating enzyme usage in metabolic reactions. It also incorporates kinetic information in the form of the turnover number (k_{cat}) of each enzyme, which is included as stoichiometric coefficients for enzyme usage in reactions. This way, reactions are constrained by the enzymatic capacities as given by the k_{cat} multiplied by the abundance of the enzyme, limiting the reaction fluxes to physiologically feasible values. Additionally, the framework allows for the integration of proteomic data.

1.6 Proteomics

An important part of systems biology is to capture the emergent properties of biological systems. With the advances in high-throughput mass-spectrometry based methods during the recent decades, proteomics, the large-scale study of proteins, has come to play an important role in systems biology [44]. Analogous to genomics and transcriptomics, proteomics denotes the study of the entire set of proteins of an organism. However, in contrast to genomics, proteomics measures the phenotype as shaped by the genotype and environmental factors [45]. From a systems biology point-of-view, proteomics contributes three different types of data. The first is expression data, that is the relative or absolute protein levels, and will be the primary proteomics data type in this thesis. Proteomics can also be used to study post-translational modifications and protein-protein interactions. In expression proteomics, much like in transcriptomics, the use of internal standards allows for absolute quantification of the proteins in a sample, which is important in some systems biology modeling frameworks. An advantage of proteomics over transcriptomics is the direct measurement of proteins, the end product of gene expressions, which are more closely related to the biological function. The quantitative nature of expression proteomics makes it very useful for comparing the phenotypic differences between samples, such as different genetic backgrounds or different experimental conditions. Furthermore, quantitative proteomics is well suited for analyzing the proteome on a subcellular level as well as creating an inventory of organellar proteomes, as has been shown by recent studies [46, 47].

1.7 Aims and significance

Until here, I have given a background of both cellular and mitochondrial metabolism (**Paper I**). I have also introduced how systems biology plays an integral role in studying metabolism due to the inherent complexity of metabolism. In this thesis, I will explore and detangle various aspects of metabolism by investigating proteome allocation and combining proteomic

data with constraint-based modeling to get an insight into metabolic fluxes. This thesis is divided into two parts. I start at the subcellular level focusing on mitochondrial metabolism, expand to cellular proteome allocation and translation, and finally analyze metabolism at the cellular level to elucidate the factors underlying the Crabtree effect.

In the first part, I focus on mitochondrial metabolism. Mitochondria are central to many cellular processes and an understanding of mitochondrial metabolism is therefore imperative to understanding cellular metabolism. In **Paper II**, I investigate the changes in mitochondrial metabolism and structure as yeast cells undergo the shift from fermentative to respiratory metabolism. I present a strategy for quantifying the proteome on a subcellular level using state-of-the-art fluorescence imaging and a precise determination of biophysical parameters. I demonstrate that mitochondria balance their role as biosynthetic hubs and centers for energy generation and that major structural and functional changes during the diauxic shift are initiated at the mitochondrial level. In **Paper III**, I constructed the first genome-scale metabolic model describing mitochondrial protein import, iron-sulfur cluster biosynthesis and the PMF in yeast. I use the model to study the dynamics and the requirement of protein import and iron-sulfur cluster biosynthesis, as well as the energy cost of transport across the mitochondrial inner membrane. The results point towards a dynamic requirement of these process, which are reported to have a rather constant expression, and the model could serve as a valuable tool for studying these processes and the implications of perturbations.

In part two, I focus on cellular proteome allocation and the importance of balancing allocation between different processes to ensure cellular function. I present a study investigating how cells' maximum capacity for growth depends on allocation of proteins to different processes (**Paper IV**). In this study, we cultivated *S. cerevisiae* in bioreactors with or without supplementing amino acids and analyzed the global changes in proteome allocation during aerobic and anaerobic growth on glucose. We found that a reallocation of protein mass, mainly from amino acid biosynthesis to translation, allowed the cells to grow faster upon amino acid supplementation. This demonstrates that proteome constraints limit cellular growth rate and by increasing the fraction of the proteome allocated to translation, cells can achieve a higher growth rate.

In the final study of part II, I put the pieces together and use the understanding gained from the first three studies to investigate the underlying causes of the Crabtree effect in yeast (**Paper V**). We cultivated four yeasts, the two Crabtree-positive *S. cerevisiae* and *S. pombe*, and two Crabtree-negative *K. marxianus* and *S. stipitis*, in bioreactors at conditions of glucose excess. We combined physiological and proteome quantification with genome-scale modeling to quantitatively describe the differences between the two groups. I demonstrate that the Crabtree effect is coupled to adaptations in metabolism, both in central carbon metabolism and translation, which reflect the trade-off between different strategies for generating ATP.

Taken together, the work in this thesis demonstrates the application of a systems biology approach combining physiological and proteome quantification with constraint-based modeling to gain insight into various aspects of metabolism.

Part I: Investigating mitochondrial metabolism

As introduced in the background section, mitochondria play an important role in a diverse set of cellular functions. Due to their importance in cellular function, mitochondrial dysfunction is implicated in various human diseases [48] and understanding mitochondrial function is therefore important to combat these diseases. The yeast *S. cerevisiae* is a widely used model organism for studying mitochondrial biology and much of our current understanding of mitochondrial function has come from studies using the yeast. In this chapter, I present two studies investigating mitochondrial metabolism. The first study (**Paper II**) investigates the role of mitochondria in the physiological and metabolic adaptations as cells shift from fermentative to respiratory growth. In the second study (**Paper III**), I present the construction of an enzyme-constrained GEM describing mitochondrial metabolism and the use of the model to study the essential mitochondrial processes of protein import and iron-sulfur cluster biogenesis as well as the effect of mitochondrial transport on the proton motive force (PMF).

2.1 The role of mitochondria in diauxic growth (Paper II)

Being Crabtree-positive, *S. cerevisiae* preferentially uses fermentative pathways for consuming glucose, which is the preferred carbon source, when glucose is available in excess. Fermentation is a high-flux process that leads to secretion of by-products, mainly in the form of ethanol, acetate and glycerol. The fermentative metabolism in presence of glucose is coupled to a repression of respiratory functions, including genes required for mitochondrial biogenesis, oxidative phosphorylation and the TCA cycle [49, 50]. As glucose is exhausted, cells undergo a transition phase, known as the diauxic shift, characterized by a metabolic reorganization from fermentation to respiration [51]. In the diauxic shift, the transition occurs gradually but is initiated as glucose availability becomes low. The shift involves a decrease in glycolytic flux, expression of glycolytic enzymes PFK and PYK, inhibition of the PPP as well as an activation of the TCA and gluconeogenesis, and is accompanied by a decrease in growth rate [52]. Some studies have investigated the changes occurring during the diauxic shift on the transcriptional level and relative changes on the cellular proteome level [52–54], as well as quantified the mitochondrial proteome on different fermentable and non-fermentable carbon sources [46, 55, 56]. However, the role of mitochondria in the switch from fermentative to respiratory metabolism is not fully elucidated. Therefore, we set out to accurately characterize the physiological adaptations by performing absolute quantification of the mitochondrial proteome and lipidome, as well as the morphology of mitochondria throughout diauxic growth in batch cultures.

2.1.1 Experimental setup

In order to study the mitochondrial morphology, we used an engineered strain of *S. cerevisiae* CEN.PK 113-7D expressing GFP and mCherry coupled to the mitochondrial targeting sequences of ATP synthase subunit 9 (preSU9) from *Neurospora crassa* and COX4 (preCOX4), respectively. preCOX4-mCherry is imported into the mitochondria strictly depending on the membrane potential, leading to import being proportional to the membrane potential. preSU9 is a strong targeting signal and can therefore drive mitochondrial import of preSU9-GFP even at low membrane potential [57]. This allows visualization of mitochondrial morphology, while at the same time ensuring the functional integrity. This strain was used throughout the study. An overview of the experimental design is given in **Figure 7**. Briefly, cells were cultivated in bioreactors in minimal medium with 2% glucose as carbon source at 30°C, pH 5 and dissolved oxygen (DO) was kept above 30%. Biological triplicates were used. Samples for proteomic and lipidomic analysis were taken at 9, 13 and 20 hours after inoculation, corresponding to fermentative metabolism, the mid-diauxic shift and respiratory metabolism, respectively. Mitochondria were isolated using differential centrifugation followed by additional sample concentration, according to [58]. The proteomes of cells and isolated mitochondria were quantified by mass spectrometry (MS) using tandem mass tags (TMT) labeling for simultaneous quantification. To obtain absolute abundances, an intensity-based absolute quantification (iBAQ) approach [59] using a reference sample spiked with the universal proteomics standard set (UPS2) protein standard. An HPLC-MS-based lipidomic analysis of crude mitochondrial extract was performed using an internal standard comprising a mixture of 15 lipid species. For characterization of mitochondrial morphology and volume of the mitochondrial network, confocal microscopy was performed. Z-stacks were generated and used to calculate the mitochondrial volume. Additionally, we performed a thorough physiological characterization by measuring cell dry weight, number and volume, as well as HPLC analysis of exometabolites.

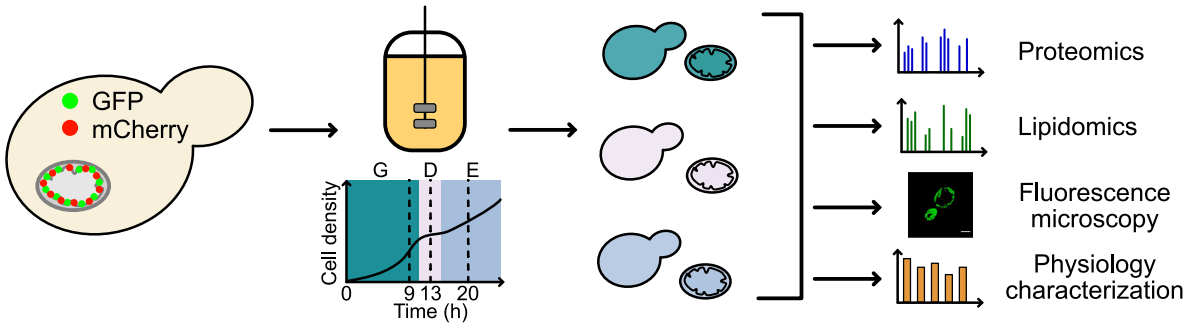

Figure 7 Overview of experimental design. Cells expressing preCOX4-mCherry and preSU9-GFP were cultivated in bioreactors in minimal medium with 2% glucose. Cells and isolated mitochondria for proteomics, lipidomics and fluorescence microscopy were harvested after 9, 13 and 20 hours. Samples for physiological characterization were taken throughout the cultivation. G, glucose phase; D, diauxic shift; E, ethanol phase

2.1.2 Quantification of cellular and mitochondrial proteome

The proteomic analysis resulted in the quantification of 3801 proteins across all whole cell samples and 3700 proteins in the isolated mitochondria samples. The high level of detected proteins in the mitochondrial fractions highlight the connectivity of the organelle but also

the high sensitivity of the MS-based approach for detection of lowly abundant contaminating proteins as seen in previous studies on the proteome of isolated mitochondria [46]. To obtain a curated set of mitochondrial proteins, we compared the proteins identified to two previous studies [46, 47] as well as the Saccharomyces Genome Database (SGD) [13]. Of the 3700 proteins identified, 1024 were annotated as mitochondrial in SGD, of which 824 were assigned through manual curation. The resulting list after curation contained 1036 mitochondrial proteins, representing a 5% increase compared to previous studies [46, 47].

2.1.3 Mitochondrial morphology

Confocal microscopy images from 50 individual cells from each replicate were analyzed and the volume of the mitochondrial network was determined. The results show that there is a large increase in mitochondrial volume as cells transition from fermentative to respiratory metabolism (**Figure 8A**). We also observed changes in the network morphology, from a small and fragmented network in the glucose phase to a more fused state in the ethanol phase (**Figure 8B**), in line with previous findings of a more interconnected mitochondrial network at conditions of growth on non-fermentable carbon sources [60]. Overall, the mitochondrial network expanded from occupying around 5% of the total cell volume in the glucose phase in the glucose phase, 11% in the diauxic shift and 35% during respiratory growth on ethanol.

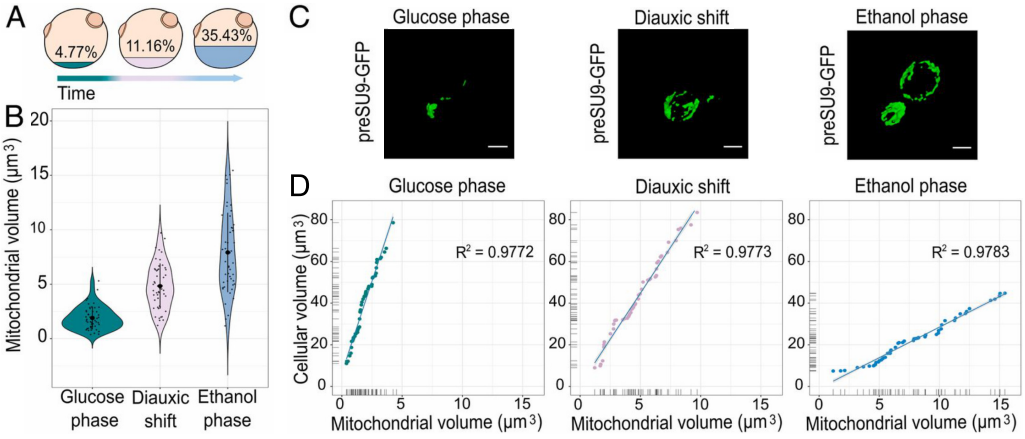

Figure 8 Mitochondrial morphology and size during the three stages of cell growth. (A) The fraction of the cellular volume occupied by the mitochondrial network. (B) The volume of the mitochondrial network as measured from 50 replicates per condition. (C) Mitochondrial morphology as determined based on confocal microscopy. Cells expressing mitochondrially targeted preSU9-GFP are shown. Scale bar, 2 μm. (D) Correlation between cell and mitochondrial volume, calculated from samples of 50 cells including budding and non-budding cells.

The mitochondrial network size is regulated in response to glucose exhaustion, starting already in the diauxic shift, suggesting a strong coupling to glucose exhaustion. In contrast to the observations on mitochondrial network size, the cell size was rather constant comparing the glucose phase and diauxic shift, and was altered only as cells start assimilating ethanol (**Figure 8C**). Furthermore, we observed a strong correlation between the cell size and the size of the mitochondrial network in all three phases. Our findings confirm the scaling of mitochondrial network size previously shown [61] and point towards mitochondria having an important role in coupling of the metabolic activity and cell size regulation in line with previous studies [62].

2.1.4 Mitochondrial proteome

To obtain a quantitative picture of the mitochondrial proteome in the three stages of growth, we set out to calculate the absolute protein abundances at the mitochondrial level. Based on previous studies on the biophysical properties of mitochondria, the density of mitochondria can be approximated as the overall density of the cell [63, 64]. We used this approximated density combined with the data on cell mass and volume, and the mitochondrial volume to calculate the mass of the mitochondrial network in the three phases. To identify the overall changes in the mitochondrial proteome as cells shift from fermentative to respiratory metabolism, we calculated the log2 fold changes (log2FC) of protein abundance between the three phases and performed significance testing using a Student's t-test. We then used a cut-off of $|\text{log2FC}| > 1$ and p-value < 0.05 to identify significantly regulated proteins (**Figure 9A-C**).

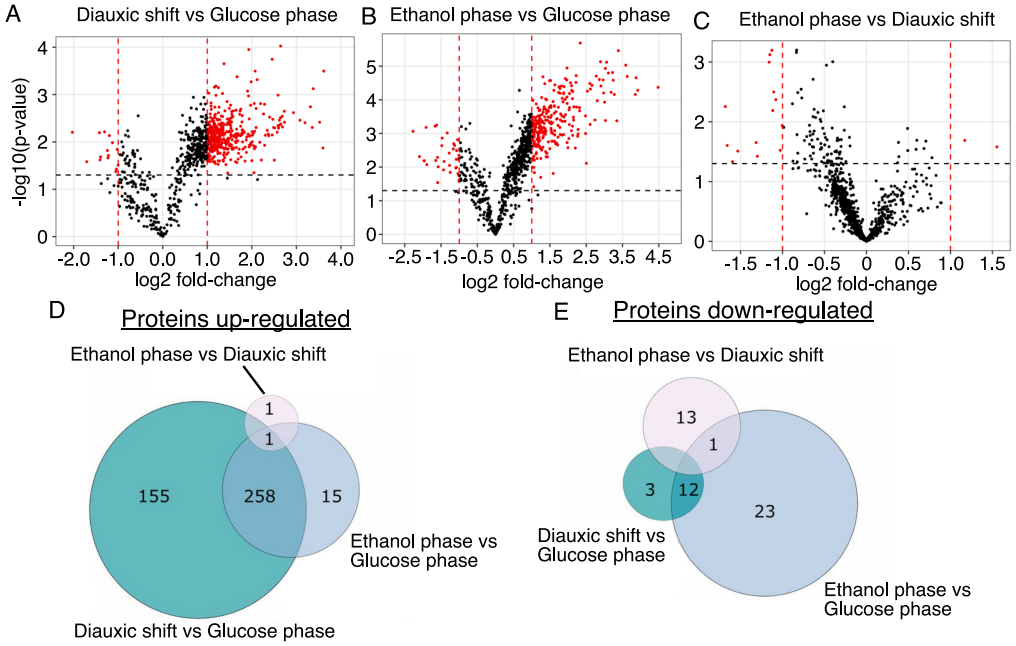

Figure 9 Changes in mitochondrial proteome composition. (A-C). Volcano plots showing the differentially expressed proteins identified after pairwise comparison of the three stages of growth. Log10 transformed p-values, calculated by a paired Student's t-test, are plotted against the log2-transformed fold change (log2FC). Vertical dashed lines indicate a fold-change cut-off of $|\text{log2FC}| > 1$. The horizontal dashed line indicates the p-value cut-off of 0.05. (D-E) Venn diagrams illustrating the number of proteins up- and down-regulated identified in the pairwise comparison between the three metabolic stages.

Overall, this resulted in the identification of 428 proteins significantly regulated comparing the diauxic shift and glucose phase (413 up and 15 down-regulated), 309 significantly regulated proteins comparing the ethanol phase and the glucose phase (273 up and 36 down-regulated), and 16 significantly regulated proteins comparing the ethanol phase and the diauxic shift (2 up and 14 down-regulated). 272 significantly regulated proteins, of which 259 were up-regulated and 13 down-regulated, were shared both when comparing the diauxic shift and ethanol phase to the glucose phase (**Figure 9D-E**). We performed a GO-term enrichment analysis for biological process using YeastMine [65] with a cut-off of Benjamini-Hochberg corrected p-value < 0.05, to elucidate trends among the proteins. We observed an enrichment of proteins in the TCA cycle, respiratory chain, ATP synthase and mitochondrial

transporters. These proteins were largely up-regulated in the diauxic shift and showed a slight further up-regulation in the ethanol phase, indicating that they are part of an early response to glucose exhaustion lasting throughout the diauxic shift. This finding has also been seen in a previous study investigating the changes in the cellular proteome during the transition from fermentation to respiration [54].

Interestingly, when performing a GO-term enrichment analysis of the proteins uniquely up-regulated comparing the diauxic shift to the glucose phase, we identified proteins involved in mitochondrial morphology and energy metabolism, further supporting the importance of regulatory events during the diauxic shift in the transition from fermentation to respiration. Furthermore, we looked into the specific set of proteins that were significantly up-regulated in the diauxic shift compared to the glucose phase but fell below the log2FC > 1 cut-off in the ethanol phase. These proteins were enriched in processes related to mitochondrial gene expression and translation, mitochondrial organization, protein targeting to mitochondria, and respiratory chain complex assembly. These findings indicate that mitochondrial biogenesis-related processes are important at an early stage of the adaptation of the mitochondrial network to respiratory growth.

2.1.5 The increase in respiration is coupled to changes in membrane architecture

The changes in respiratory processes observed when analyzing the mitochondrial proteome led us to further investigate proteins involved in respiration. It has been established that the mitochondrial membrane architecture is tightly linked to mitochondrial function, and respiratory chain complexes and ATP synthase have been shown to be enriched in folds in the inner membrane referred to as cristae [66]. Therefore, we also focused the analysis on cristae-associated proteins including the components of the respiratory chain, and the mitochondrial contact site and cristae organizing (MICOS) complex involved in cristae organization [67]. Overall, we observed a 3.5-fold increase in the abundance of cristae-associated proteins comparing the diauxic shift to the glucose phase and an additional 0.3-fold increase as cells progressed into the ethanol phase (**Figure 10A**). This suggests that there are clear changes, not only in the size of the mitochondrial network as shown in **Figure 8B**, but also the organization of the mitochondrial inner membrane in response to an increase in respiration.

The increase in the overall abundance of cristae-associated protein was further reflected in the abundance of the individual components of the respiratory chain and ATP synthase (**Figure 10B and C**). The complexes show a significant, roughly 3-fold, increase in abundance as the cells enter the diauxic shift and, in line with what was observed at the overall mitochondrial proteome level, show only a slight increase in abundance comparing the ethanol phase to the diauxic shift. This confirms previous findings that these processes are part of an early response in the shift from fermentation to respiration.

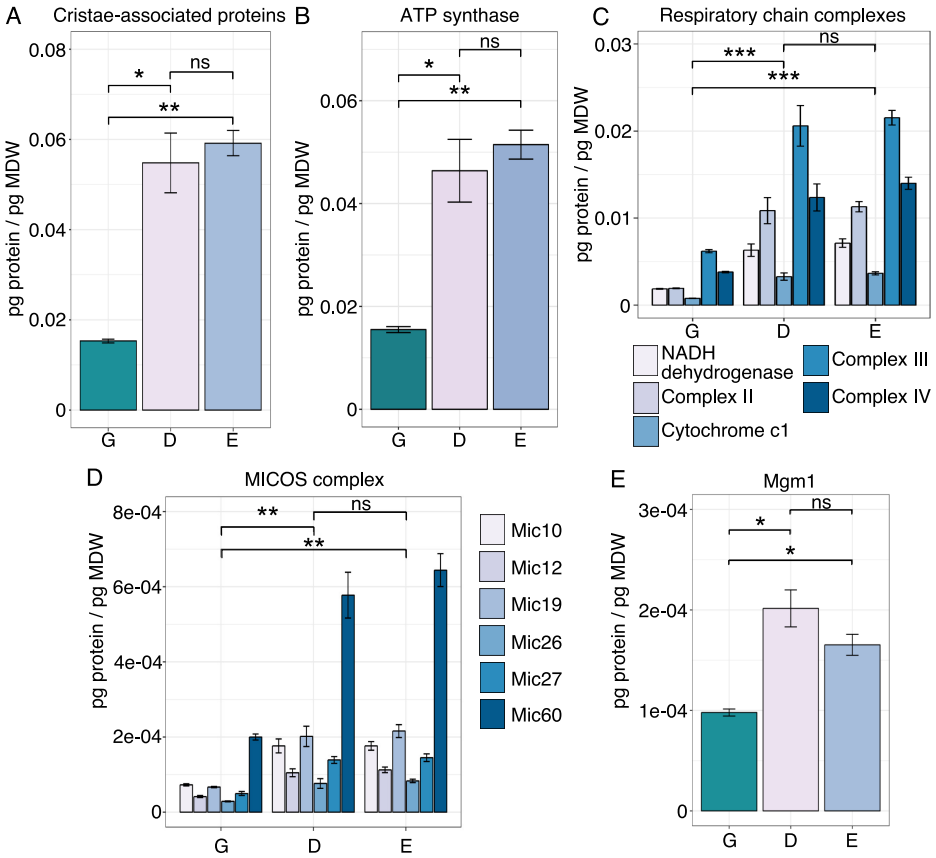

Figure 10 Increasing proteome allocation of respiratory proteins is coupled to changes in cristae formation. Absolute protein abundances of cristae-associated proteins (A), ATP synthase (B), respiratory chain complexes (C), mitochondrial contact site and cristae organization (MICOS) complex components (D) and dynamin-like GTPase Mgm1 (E). Data represent mean values ± standard deviation of three biological replicates. Statistical comparisons were performed using paired t-test. ns, not significant ($p > 0.05$); $*p < 0.05$; $**p < 0.01$; $***p < 0.001$. G, glucose phase; D, diauxic shift; E, ethanol phase.

The respiratory chain and ATP synthase have been shown to assemble into supercomplexes (SCs) within the cristae of the mitochondrial inner membrane and the cristae structure directly affects the assembly and stability of these complexes [68]. The MICOS complex is located at cristae junctions, where it has been shown to regulate membrane architecture through stabilizing cristae curvature [69]. In addition to the MICOS complex, the mitochondrial GTPase Mgm1, has been shown to play a critical role in maintenance of cristae structure, as well as in assembly and stability respiratory chain SCs [68, 70]. In our proteomic data we observed a 3.5-fold and 2-fold increase in abundance for the MICOS complex and Mgm1, respectively after the transition from the glucose phase to the diauxic shift, followed by a similar abundance in the ethanol phase (**Figure 10D and E**). Overall, the findings from the analysis of the respiratory chain, ATP synthase and proteins involved in maintaining the membrane architecture support the hypothesis that the structural and functional changes of mitochondria occur in the diauxic shift to prepare cells for respiratory metabolism as glucose is exhausted.

2.1.6 Remodeling of the mitochondrial inner membrane

Given the observed changes in inner membrane architecture, we performed an analysis of the lipidome of isolated mitochondria to investigate the coupling of the increase in respiration to the composition of the inner membrane. Here, I will focus on the observations

for the mitochondrion-specific phospholipid cardiolipin (CL). As mentioned in the background section, CL is a phospholipid consisting of four acyl chains connected to a dimeric glycerophosphate backbone, giving the phospholipid a conical shape suitable for areas of membrane curvature. Furthermore, it has been implicated in stabilizing individual complexes of the respiratory chain [38]. Comparing the abundance of CL in the three stages of growth, we observed an increase in the levels in the diauxic shift compared to the glucose phase followed by a decrease in abundance as cells entered the ethanol phase (**Figure 11A**). In addition to the increase in abundance of CL as cells transition to respiratory metabolism, we also observed a change in the level of unsaturation of the phospholipid (**Figure 11B and C**). As respiration increased, we observed an increasing preference for incorporation of unsaturated acyl chains in CL, resulting in an increase in the overall degree of unsaturation. An increase in acyl chain unsaturation in CL has been speculated to increase the fluidity in the cristae membrane regions, in turn leading to an increased curvature and incorporation of ATP synthase complexes [38]. The increase in unsaturation seen is in line with a previous study linking an increase in membrane viscosity through increased unsaturation to increased respiratory activity [71], further highlighting the importance of membrane architecture in promoting respiratory metabolism.

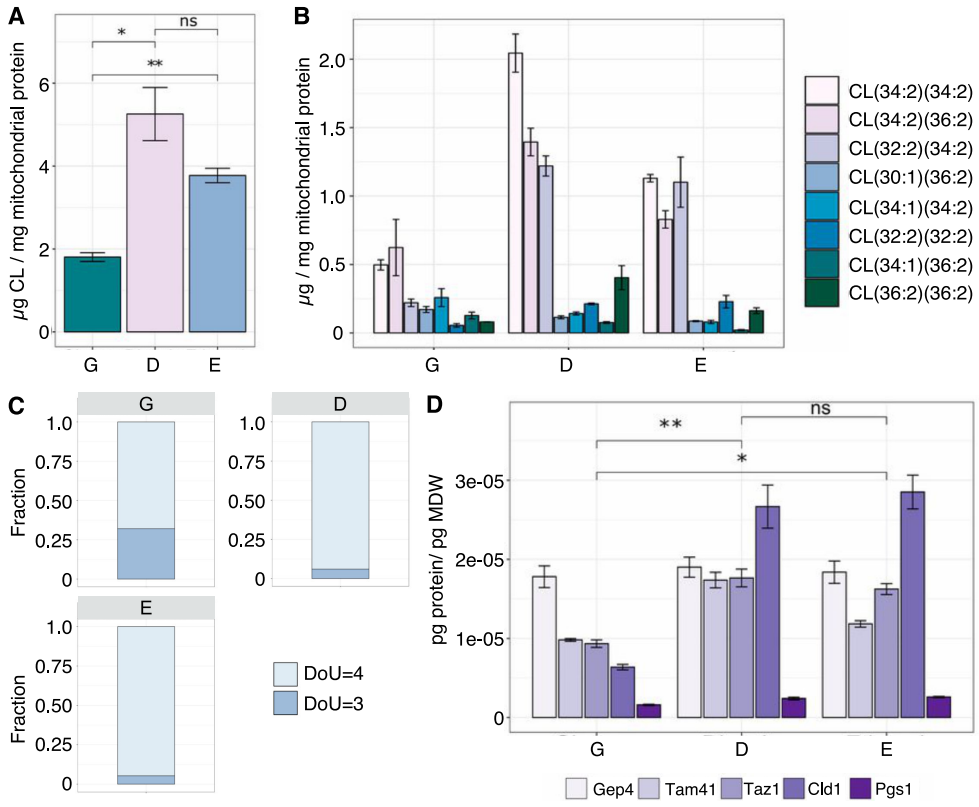

Figure 11 Changes in abundance and unsaturation of cardiolipin. (A) Abundance of cardiolipin (CL). (B) Absolute abundances of individual CL species. (C) Degree of unsaturation (DoU) of total CL species in the three stages of growth. (D) Absolute abundances of proteins involved in CL biosynthesis. Statistical comparison was performed using paired t-tests. Significance levels are defined in the following way: not significant (ns), $p > 0.05$; $*p < 0.05$; $**p < 0.01$. G, glucose phase; D, diauxic shift; E, ethanol phase.

The changes observed in CL unsaturation were also reflected in the abundances of proteins involved in CL biosynthesis (**Figure 11D**). We observed an increase in abundance of the phospholipase Cld1 and acyltransferase Taz1, the main enzymes responsible for maturation of CL through remodeling of the acyl chains. Cld1 removes an acyl chain, preferably C16:0, from premature CL to form an intermediate monolysocardiolipin (MLCL), and Taz1 subsequently catalyzes the acylation of MLCL to form mature CL [72, 73]. We observed an up-regulation of both the enzymes in the diauxic shift compared to the glucose phase, while maintaining similar enzyme levels in the ethanol phase. This further highlights the diauxic shift as an important stage for remodeling of the mitochondrial network.

2.1.7 The dual role of mitochondria in cellular metabolism

To analyze the overall changes in mitochondrial proteome allocation as cells shift from fermentation to respiration, we divided the proteome into 19 groups based on protein function and compared the allocation between the two stages (**Figure 12A**). Three main trends were observed. The first trend was the significantly higher allocation of energy-related processes, including the TCA cycle, respiratory chain and ATP synthase during respiration, as previously observed. Second, we observed a lower allocation for biosynthetic processes, including biosynthesis of amino acids, cofactors, sterols and phospholipids. Lastly, the allocation of processes related to mitochondrial biogenesis, including the protein import machinery, and the related chaperones and proteases, as well as maintenance of the mitochondrial genome, have a similar allocation in fermentation and respiration. This is an interesting finding since the protein import machinery imports more than twice the amount of protein during respiration [74] and is therefore something we explored further in **Paper III**.

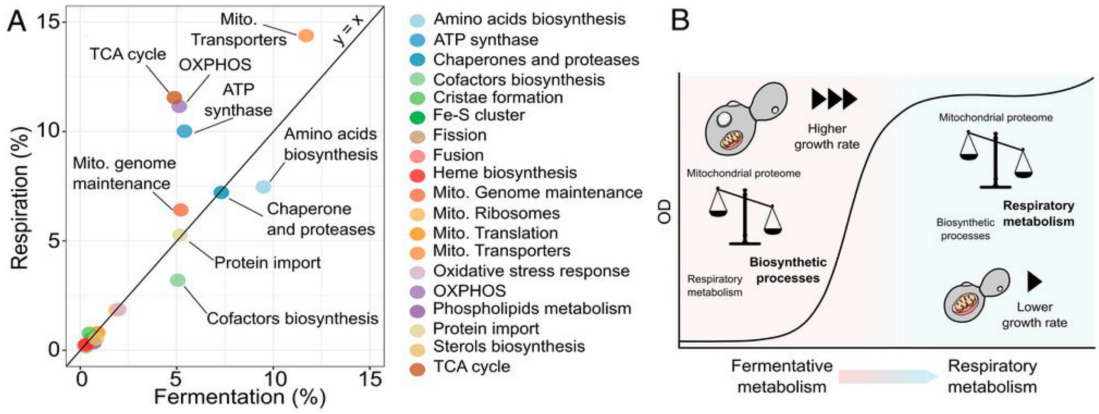

Figure 12 Dual role of mitochondria in cellular metabolism. (A) Comparison of the allocation of the mitochondrial proteome during respiration and fermentation. (B) Overview of the shift in the role of mitochondria in metabolism from a biosynthetic hub during fermentation to a center for energy generation during respiration.

In summary, we showed that mitochondria play a dual role in metabolism, serving as a biosynthetic hub during fermentation while shifting towards an energy generation-centered role during respiration, as visualized in **Figure 12B**.

2.2 Modeling mitochondrial metabolism (Paper III)

Mitochondria have gained an increasing interest due to the numerous important physiological functions and the number of human disorders linked to mitochondrial dysfunction [75]. With advances in proteomic, genomic and bioinformatic approaches for studying mitochondria, there is now an ever-increasing inventory of mitochondrial components [76]. Given the complexity of metabolism, a systems level understanding can be aided by using computational models, which lie at the heart of systems biology [3]. Owing to the genetically and biochemically consistent format of the computational models, especially genome-scale models, for representing metabolic networks, they represent valuable scaffolds for integrating omics data with the added benefit of improving model predictions [77, 78].

So far, several stoichiometric models of human mitochondrial metabolism have been developed. The first detailed model was constructed by Vo and co-workers, and described energy metabolism, detoxification of reactive oxygen species (ROS), synthesis of heme, as well as lipid and nitrogen metabolism in human cardiac mitochondria [79]. The model proved useful for determining the ATP yield per glucose, as well as providing insight into the flexibility of lipid and heme production. It was later used to study mitochondrial metabolism under different metabolic conditions, including diabetic and ischemic conditions [80]. A more recent model of human mitochondria was constructed by Smith and Robinson in 2011 [81]. The model was used to study metabolic disorders related to the TCA cycle. It was later expanded and used for simulating respiratory chain disorders, and more recently also expanded to a more comprehensive representation of central metabolism [82, 83]. Although these models have proven useful, as these models do not directly account for enzymes, they are limited to studying the turnover of metabolites within the mitochondrial metabolic network. Another common feature of these models is that they are limited to central metabolism. Connecting enzymes to metabolism would allow for studying the dynamics of the mitochondrial proteome under different conditions, which in turn would aid our understanding of mitochondrial function. Furthermore, integrating mitochondrial metabolism in overall cellular metabolism would allow studying the interactions of mitochondria with other metabolic processes.

In **Paper III**, we constructed an enzyme-constrained model of mitochondrial metabolism in the model eukaryon *S. cerevisiae*, which has served as an important model for studying mitochondrial function. The model encompasses a detailed representation of mitochondrial protein import and Fe-S cluster biogenesis, two processes that are essential for cellular function in all conditions. We introduced a detailed representation of the proton motive force (PMF) to directly link transport reactions and the respiratory chain to ATP synthesis. Additionally, we represented the incorporation of the cofactors biotin, lipoic acid, Fe-S clusters and heme into enzymes.

2.2.1 Model reconstruction

The model was created using the consensus yeast GEM as a scaffold [84], with two new mitochondrial compartments, the intermembrane space and outer membrane added. The

model was generated using the GECKO framework for incorporating enzymatic constraints in metabolic models [43, 85]. This culminated in ecMitoYeast, which is outlined in **Figure 13A**. As a consequence of describing mitochondrial enzyme requirements as well as import of proteins and cofactor incorporation, the newly reconstructed content resulted in a change in enzyme usage from an amount in the unit mmol/gDW to a flux with unit mmol/gDW/h (**Figure 13B**). To balance the units of enzyme exchange reactions, the growth rate is accounted for in the stoichiometric coefficients of enzyme usage in the reactions. This also meant that simulations using the model were performed using a binary search to find the maximum feasible growth rate. In the following sections, I will go through the procedure of reconstructing the added content in more detail as well as present the main findings from the related model simulations.

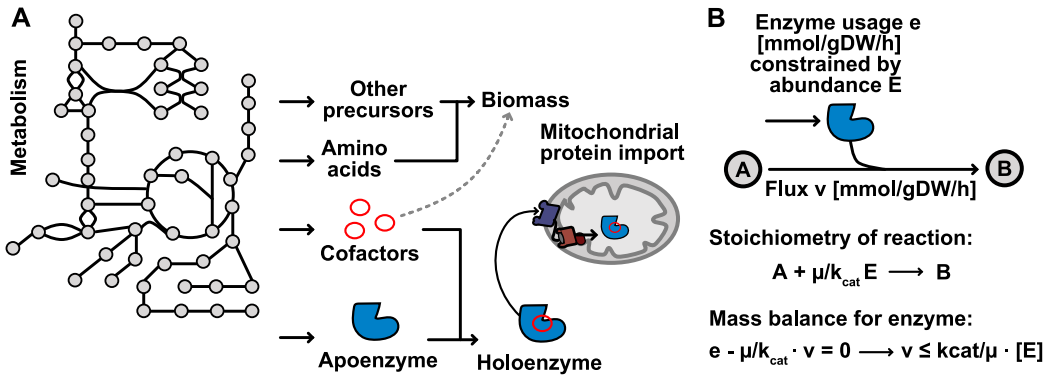

Figure 13 Overview of the ecMitoYeast model. (A) Scope of the model. In addition to metabolism, the model accounts for cofactor biosynthesis and binding to enzymes, and the translocation of proteins into mitochondria. The dotted line signifies the inclusion of cofactor requirement of unmodeled proteins into the biomass reaction. (B) The relationship between metabolic reaction and enzyme usages established based on a steady-state assumption.

2.2.2 Modeling the proton motive force

The PMF, as described earlier in this thesis, is generated by the translocation across the mitochondrial inner membrane at complexes III and IV of the respiratory chain, upon the transport of electrons originating from NADH or $FADH_2$ through the ETC. It consists of two components, a membrane potential ($\Delta\Psi$) arising from the difference in charge, and a proton gradient (ΔH^+) resulting from the difference in proton concentration across the membrane [86]. The PMF is not only affected by the translocation of protons in the ETC, but also by other processes transporting charge and/or protons across the inner membrane such as metabolite transport and protein translocation. As the PMF is central for mitochondrial function, we set out to represent it in the model. Inspired by a model of human cardiac mitochondria [83], we implemented an approach where a pseudometabolite representing the PMF is introduced in the model. This metabolite was set to be co-transported in reactions transporting charge or protons across the membrane. A relative contribution of ($\Delta\Psi$) and (ΔH^+) of 0.9 and 0.1, respectively, was used based on experimental data [87], using the average value from experiments with NADH and ethanol as substrates. Accordingly, the complexes of the ETC and ATP synthase move PMF pseudometabolites corresponding to the number of protons translocated (**Figure 14A**). As two examples of transport reactions the ATP/ADP translocase transporting a net negative charge across the membrane was

set to co-transport 0.9 PMF and the electroneutral, but proton-translocating phosphate transporter was set to co-transport 0.1 PMF pseudometabolites (**Figure 14B**).

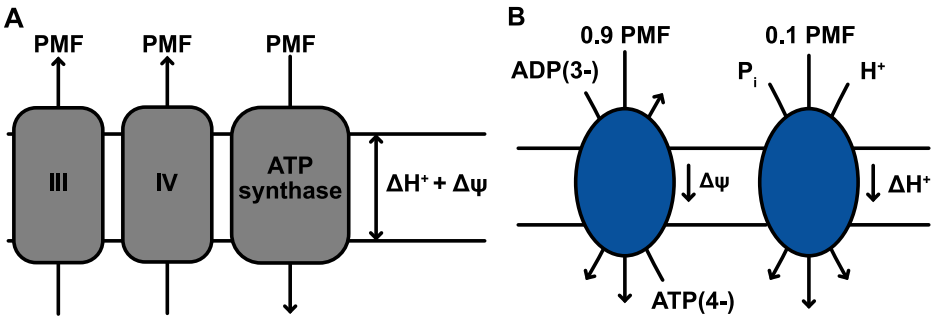

Figure 14 Representation of the PMF in the model. (A) Coupling of the respiratory chain complexes and ATP synthase to the proton motive force (PMF). The components transfer PMF corresponding to the number of protons translocated across the inner membrane. (B) Coupling of reactions transporting charges or protons across the inner mitochondrial membrane to the PMF as exemplified by the ADP/ATP translocase, resulting in net transfer of a negative charge, and electroneutral but proton coupled phosphate carrier.

We evaluated the effect of modeling the PMF on model performance by comparing the phosphate-oxygen ratio (P/O) in our model to a model without the PMF represented simply using the theoretical P/O of 1.5. The P/O was calculated as the ratio between the ATP production and the number of electron pairs entering the ETC at the NADH dehydrogenases and complex II and was found to be 1.08 (**Figure 15A**). This value is close to the experimentally determined P/O of approximately 0.95 [88]. Based on these results, a PMF sink was introduced in the following simulations and constrained to a value bringing the operational P/O ratio closer to the *in vivo* value. Furthermore, we evaluated the energy cost explicitly represented by metabolite transport. We calculated the change in the growth-associated energy cost (GAEC), that represents a combination of processes related to growth not associated to polymerization of macromolecules, by fitting to experimental data and compared the resulting cost to that in a model without the PMF represented. We observed a decrease in the simulated GAEC from 49.1 to 17.1 mmol ATP/gDW. Metabolite transport across the mitochondrial inner membrane was calculated to account for 27% of the total PMF generated at a growth rate of 0.1 h^{-1} (**Figure 15B**).

We next ran simulations at increasing growth rates to evaluate the P/O ratio and biomass yield (**Figure 15C**). We found that the P/O ratio was rather constant at the different growth rates, the exceptions being at maximum growth rate both with glucose and ethanol as carbon source. The model correctly predicted a drop in biomass yield at higher growth rates seen experimentally [89]. Our findings demonstrate that representing the PMF in the yeast model improves performance by directly accounting for a significant energy cost that was previously lumped together into the GAEC but can now be estimated and evaluated using the model.

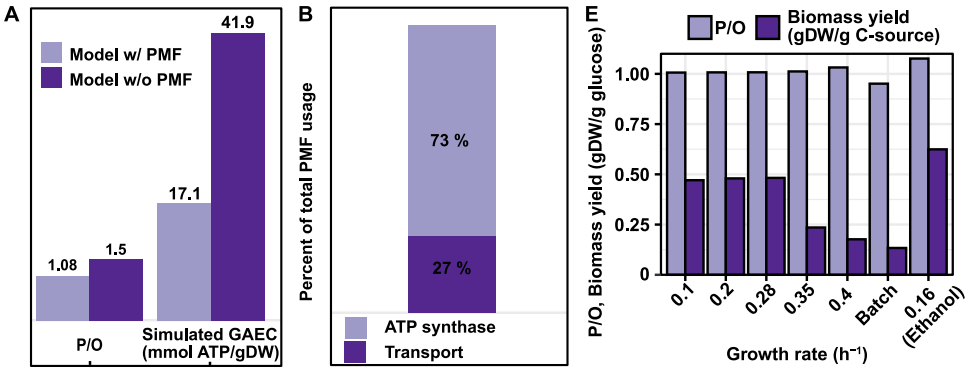

Figure 15 Effect of representing the PMF in the model. (A) Effect of explicitly modeling the PMF on the operational phosphate/oxygen ratio (P/O) and the simulated growth-associated energy cost (GAEC). (B) Overall fraction of the generated PMF used for transport across the inner membrane, and synthesis of ATP. (C) P/O ratio and biomass yield on carbon source at increasing growth rate. Unless otherwise specified, glucose was used as carbon source. The ethanol condition represents conditions of maximum specific growth rate.

2.2.3 Modeling mitochondrial protein import

Roughly 99% of the mitochondrial proteins are synthesized by cytosolic ribosomes and therefore must be imported into the correct mitochondrial compartment. Depending on the final localization of the proteins, five main pathways for import exist [90]. Since the scope of our model was on metabolism, we focused on three of these pathways (**Figure 16A**), namely (i) import of IMS proteins through the mitochondrial intermembrane space assembly (MIA) complex [91], (ii) translocase of the inner membrane 22 (TIM22) complex-mediated pathway for inner membrane proteins and (iii) the translocase of the inner membrane 23 (TIM23) mediated pathway for import of proteins into the mitochondrial matrix and inner membrane. The remaining two pathways include the import of outer membrane proteins, that are mostly out of the scope of the model, by the sorting and assembly machinery (SAM) [92], and the mitochondrial import complex (MIM) [93], for which mechanistic knowledge is scarce. The main pathway of import is the TIM23 pathway, which is responsible for import of 60-70% of all mitochondrial proteins [94]. These proteins are synthesized with a cleavable N-terminal targeting sequence of around 15-50 amino acids in length, directing the proteins to the mitochondrion, that is cleaved by mitochondrial processing peptidase (MPP) upon import. Import occurs through the action of the translocase of the outer membrane (TOM) and TIM23 assisted by the presequence translocase-associated motor (PAM). The presequences are positively charged and are imported through TIM23 driven by $\Delta\Psi$ [57]. Thereafter, the mechanism depends on the final destination of the protein. Matrix proteins are further translocated driven by multiple cycles of ATP binding and hydrolysis by mitochondrial Hsp70 associated to PAM. Most inner membrane proteins contain a hydrophobic sorting signal causing translocation to halt and directing insertion into the membrane [95]. A few inner membrane proteins are fully translocated into the matrix and then inserted into the membrane by the oxidase assembly (OXA), also responsible for insertion of proteins synthesized by the mitochondrial ribosome [96]. Although the model does not account for the mitochondrial carrier proteins, we chose to include the TIM22 machinery responsible for import of the carrier proteins [97] based on it being responsible for import of some of the components of TIM23.

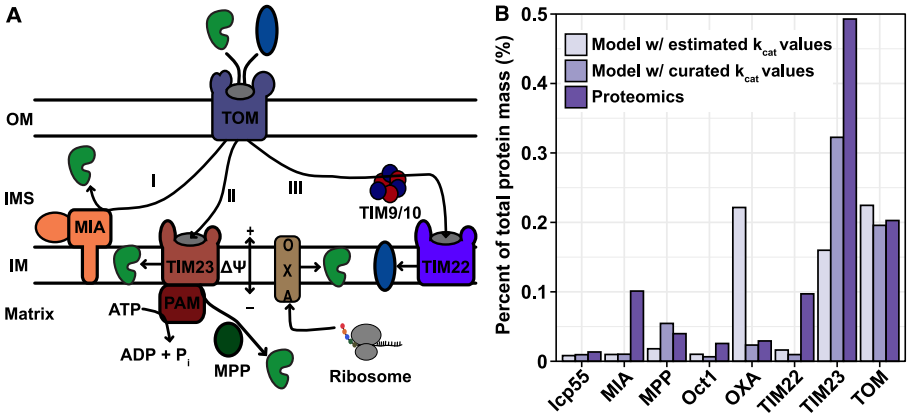

Figure 16 Modeling protein import. (A) Overview of the pathways incorporated in the model. (I) The disulfide relay pathway mediated by MIA for import of IMS proteins, (II) The TIM23-mediated pathway for import of proteins synthesized with a cleavable N-terminal sequence, and (III) the TIM22-mediated pathway for import of mitochondrial carrier proteins. (B) Validation of model performance. Predicted allocation of the components of mitochondrial protein import compared to allocation as measured by proteomics [98]. OM, outer membrane; IMS, intermembrane space; IM, inner membrane; TOM, translocase of the outer membrane; MIA, mitochondrial import and assembly; TIM23, translocase of the inner membrane 23; PAM, presequence translocase-associated motor; MPP, mitochondrial processing peptidase; OXA, oxidase assembly; TIM22, translocase of the inner membrane 22.

We used the wealth of knowledge available in the literature to reconstruct protein import. As a first step, all proteins were assigned to a compartment based on the localization evidence available in SGD and the MitoMiner database [76], which incorporates localization evidence from UniProt, mass spectrometry- and GFP studies, as well as presequence predictions and gene ontology information. We then used the compiled evidence to assign each model protein to a compartment and a translocation pathway. Template reactions were constructed for each import pathway and were then used to add the import reaction for individual proteins. As an example, the template reaction for the TIM23 pathway of matrix import is:

$$\begin{aligned}&\text{protX[c]} + y\text{PMF[ims]} + x\text{ATP[m]} + x\text{H2O[m]} => \\ &\quad \text{protX[m]} + y\text{PMF[m]} + x\text{ADP[m]} + x\text{phosphate[m]} + x\text{H}^{+}\text{[m]} + \text{presequence[m]} \end{aligned} \quad (2.1)$$

where y represents the effect on the PMF as calculated from the total charge of the protein. x is the number of ATP required for import calculated using the protein sequence length and an average length between binding sites of mtHsp70 of 25 amino acids, resulting in 1 ATP per 25 amino acids [99]. As an initial step in adding the usage of protein import complexes to the import reactions, we estimated the k_{cat} values based on proteomics data [100], given the assumption that protein degradation can be neglected, as:

$$k_{\text{cat}} = \mu * \frac{\Sigma[E]}{[E]} \quad (2.2)$$

where μ is the specific growth rate, Σ[E] is the summed abundance of proteins requiring the import complex and [E] is the mean abundance of complex subunits. To validate the model performance, we compared the model simulated proteome allocation of the import components at a dilution rate of 0.1 h^{-1} to experimentally measured abundances [98] (**Figure 16B**). The correlation between measured and model predicted protein abundances was not

significant (Pearson's R = 0.53, p-value = 0.17). To improve the model performance, we queried the BRENDA database [101], as well as the available literature for k_{cat} values. Curating the k_{cat} values with experimental data, and substituting the proteomics-estimated k_{cat} values for measured k_{cat} values when available, resulted in a significant correlation between measured and model predicted protein abundances (Pearson's R = 0.73, p-value = 0.039). The two main outliers were MIA and TIM22, which can be explained by the fact that many of the protein substrates of MIA functioning in copper homeostasis and respiratory chain complex assembly in the case of MIA and metabolite transport in the case TIM22, processes that are outside the scope of our model.

We also analyzed the levels of protein import components at increasing dilution rates, from 0.1 h^{-1} to 0.4 h^{-1}, and at maximum growth rate (**Figure 17A and B**). We observed an increase in the fraction of the proteome allocated to protein import up to the critical dilution rate for fermentation onset at 0.28 h^{-1}, from 0.63% at 0.1 h^{-1} to 1.67% at 0.28 h^{-1}, while the allocation based on proteomics data was 1% at 0.1 h^{-1}. At higher growth rates, the allocation decreased, in line with an increase in fermentation, reaching an allocation of 0.47% at maximum growth rate. Interestingly, the allocation at 0.4 h^{-1} was higher than at 0.1 h^{-1}, pointing towards the respiratory activity required to support the respiro-fermentative metabolism at high growth rates is higher than that required at fully respiratory metabolism at low growth rates.

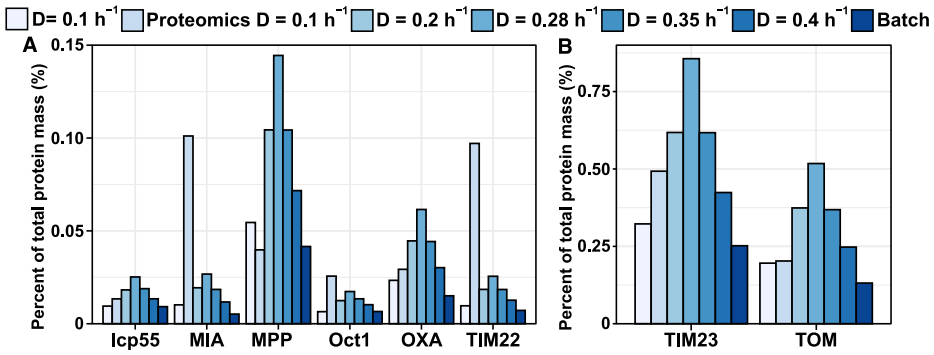

Figure 17 Modeling protein import. Model-predicted requirement of the protein import machinery at increasing dilution rates and at maximum growth rate, compared to allocation from proteomics data at dilution rate 0.1 h^{-1}.

Protein import has been shown experimentally to occupy around 5% of the mitochondrial proteome both during fermentation and respiration (**Paper II**, [46, 74]). The mitochondrial proteome accounts for around 10% and 20-30% of the cellular proteome in fermentation and respiration, respectively. Protein import would therefore account for 0.5% and 1.5% of the cellular proteome in fermentation and respiration respectively, which is in good agreement with the model predictions. However, it should be noted that ecMitoYeast covers metabolic proteins, which correspond to roughly 2/3 of the mitochondrial proteome by mass.

2.2.4 Modeling cofactor biosynthesis and incorporation

Mitochondria are involved in the synthesis of a variety of cofactors, including lipoic acid, biotin, iron-sulfur clusters and heme. The functions of these cofactors range from mitochondrial α-keto acid dehydrogenases and respiratory proteins to carboxylases and enzymes in amino

acid biosynthesis. Therefore, mitochondrial cofactor biosynthesis is important for the overall function of the cell and iron-sulfur cluster biosynthesis is one of the essential mitochondrial processes under any given condition. An accurate representation of cofactor biosynthesis is imperative for a model of mitochondrial metabolism. We constructed reactions for the synthesis of Fe-S clusters representing the three distinct steps as illustrated in **Figure 5** as well as reactions for synthesizing lipoic acid. The enzymes responsible for the synthesis of the cofactors were also included in the model. Thereafter, we constructed a list of enzymes containing the above mentioned cofactors using information available in the literature and the UniProt database [102]. Based on this list, we added reactions for incorporating cofactors into enzymes for enzymes included in the model and added a cofactor requirement in the biomass reaction for the non-modeled enzymes (**Figure 13A**).

To investigate the changes in cofactor usage, we used the model to estimate the cofactor requirements at increasing growth rate in the span of 0.1-0.4 h^{-1} and maximum growth rate (**Figure 18A-C**). We observed three different trends for the cofactor requirements. First, the requirement of biotin and siroheme scaled with growth rate, displaying the highest requirement at maximum growth rate. This can be explained by the proteins requiring these cofactors being involved in biosynthetic processes, thus causing an increased requirement as the requirement for biomass precursors increases. For example, siroheme is required for the function of Met5 involved in methionine biosynthesis, and biotin is required for the function of Acc1 and Hfa1 in fatty acid biosynthesis. Second, the predicted requirement for ferroheme b, lipoic acid and [2Fe-2S] clusters scaled with the respiratory activity with a maximum requirement at 0.28 h^{-1} before the onset of fermentation. A decrease in the requirement was observed after that point, in line with most of the proteins requiring these cofactors being respiratory proteins or proteins of the TCA cycle. Lastly, the requirement of heme A and [4Fe-4S] clusters showed a dual dependence on the growth rate and respiratory activity. The requirement increased with the respiratory activity, with a maximum requirement at 0.28 h^{-1}, and largely retained the level after the onset of fermentation, highlighting the dual function of these cofactors in respiration and biosynthesis.

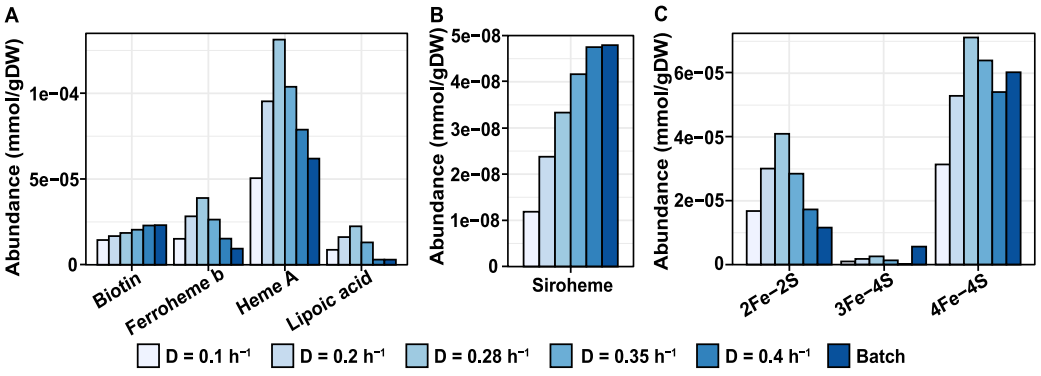

Figure 18 Cofactor requirements at increasing growth rate. Absolute requirements predicted by the model for (A) biotin, ferroheme b, heme a and lipoic acid, (B) siroheme, and (C) iron-sulfur clusters.

In conclusion, we constructed a detailed model of mitochondrial metabolism, comprising a representation of the PMF, protein import and cofactor metabolism. Our work provides insight into the dynamics of mitochondrial metabolism. Our model could serve as a valuable

tool complementing experimental work, and given the high conservation of mitochondrial metabolism, could also be valuable for studying mitochondrial dysfunction related to human diseases.

Part II: Investigating constraints in cellular metabolism

As seen in part I of this thesis, changes in the growth conditions lead to changes in the allocation of the cellular proteome resources in order for the cell to adapt its finite resources to the environmental conditions given. The principles behind cellular resource allocation have been given extensive attention in recent years, as developments in high-throughput techniques have allowed for quantification of gene expression and protein abundances. An important step in the resource allocation theory was the realization that the cost of making enzymes was in itself an important factor determining the growth rate of cells [26]. This led to the consideration of cells as self-replicating systems that, in order to proliferate, need to duplicate their components before the next cell division. To do so, the cell needs to use its metabolic pathways to break down substrates into building blocks for polymerization of macromolecules that make up the cell. The balance between the fluxes from metabolic precursors to polymerization determines the growth rate. Cells have to make a substantial investment in the machinery, mainly in ribosomes, responsible for polymerization and at the same time also in the enzymatic machinery catalyzing metabolic reactions. Given the finite proteome resources, cells need to balance the investment in different cellular processes. In models of resource allocation, this balance is studied by dividing the proteome into fractions, which are used to derive growth laws [103]. Studies performed by perturbing the metabolism of *Escherichia coli*, demonstrated that the proteome could be divided into sectors based on how the expression of the proteins within a sector responded upon perturbations of metabolism [103, 104]. The importance of resource allocation in determining cellular phenotypes has been further demonstrated in studies of nutrient limitations and overflow metabolism in *E. coli* [105, 106], as well as studies on the effect of different carbon sources on the growth of *S. cerevisiae* [25]. A common theme in these studies was the perturbation of metabolism by imposing limitations, such as carbon- and nitrogen limitation or partially inhibiting translation, causing a lowered growth rate. In this chapter, I present two studies that aim to expand the current knowledge on how constraints in metabolism, mainly arising from finite proteome resources, affect cellular phenotypes. In the first study (**Paper IV**), we cultivated *S. cerevisiae* under the supplementation of amino acids and studied the effect on growth rate and proteome allocation. In the second study (**Paper V**), we investigated the underlying causes of the Crabtree effect, which has been suggested to arise from limitations in proteome resources.

3.1 Proteome allocation upon supplementation of amino acids (Paper IV)

In this study, we evaluated the effect of supplementing amino acids on the growth and proteome allocation of yeast. An overview of the experimental setup is given in **Figure 19A**. Briefly, we cultivated *S. cerevisiae* CEN.PK 113-7D in bioreactors in minimal medium with 2% glucose as carbon source. We tested four different conditions, combining aerobic and anaerobic conditions with or without the supplementation of a mix of 14 amino acids commonly used in protein production medium [107]. We used an LC-MS/MS-based approach consisting of tandem mass tags (TMT) and intensity-based absolute quantification (iBAQ) [59] using a UPS2 protein standard-spiked reference sample, to measure the absolute protein abundances in the four conditions. We also measured the concentration of biomass, amino acids and exometabolites throughout the cultivations. An overview of the proteomic analysis is given in **Figure 19B**. In total, we quantified the abundance of 3690 proteins all samples combined, of which 3074 (83%) were identified in all samples. The largest variation was seen between the samples from aerobic and anaerobic cultivations, where 206 and and 404 proteins, respectively, were identified in only one of the conditions. The difference between these conditions were also reflected in the principal component analysis (PCA), showing that the samples cluster according to the oxygen supply (**Figure 19C**).

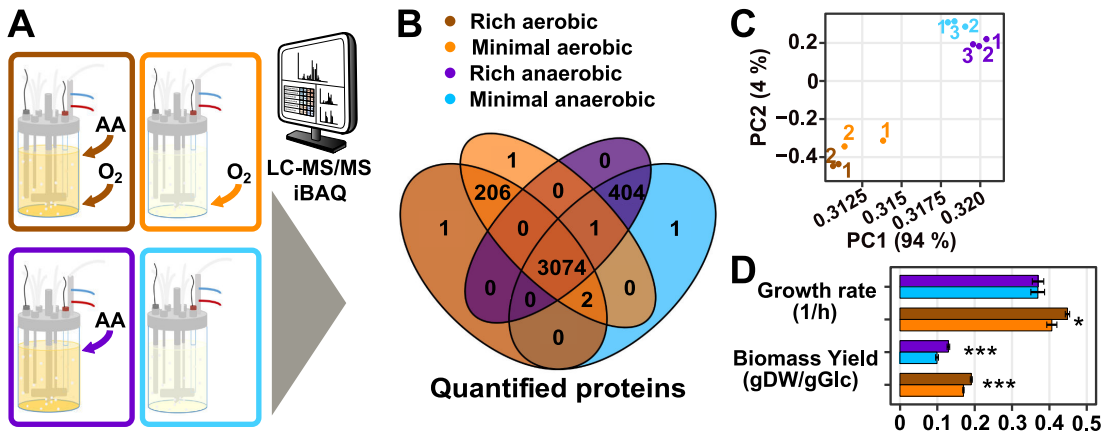

Figure 19 Overview of experimental setup and general findings. (A) *S. cerevisiae* was cultured in minimal media with 2% glucose in aerobic and anaerobic conditions with or without the supplementation of amino acids. Proteome quantification was performed using intensity-based absolute quantification (iBAQ). (B) Venn diagram showing the overlap between samples for the 3690 proteins quantified in total. (C) Principal component analysis (PCA) plot of the protein abundances showing the clustering of samples based on oxygen availability. (D) Growth rate and biomass yield.

3.1.1 Amino acid supplementation allows cells to grow faster

The analysis of the biomass concentration showed that the cells grow faster when supplementing amino acids and that the biomass yield was higher in both aerobic and anaerobic conditions (**Figure 19D**). For anaerobic conditions, the increased growth rate was not seen from the biomass measurements, but when calculating the growth rate based on the carbon dioxide production profile we found that the growth was faster when supplementing amino acids. This indicates that supplementing amino acids to the medium has a direct effect on the proteome constraints limiting growth. To investigate the effect of adding amino acids, we first

quantified the amino acid uptake by measuring the amino acid concentrations in the medium at different time point throughout the cultivation, and compared it to the requirement of amino acids for formation of biomass as defined in the yeast consensus GEM [84] (**Figure 20A**). Overall, the amino acid uptake was similar in the two conditions studied and most amino acids were taken up in an amount similar to the biomass requirements. However, we observed a higher uptake of methionine, arginine and threonine. For arginine and threonine, we observed an increase in the abundance of enzymes involved in catabolizing the amino acids. In the case of arginine, the two catabolic enzymes, Car1 and Car2, converting arginine into proline as well as Dur1,2 involved in the conversion of arginine to urea were significantly up-regulated. This indicates that arginine is used both as a source of nitrogen and a precursor for proline synthesis. We also observed a down-regulation of the enzymes responsible for synthesizing arginine. These findings are in line with previous studies showing that excess cytosolic arginine leads to an induction in expression of Car1 and Car2, and a repression of Arg1 and Arg3 in arginine synthesis [108, 109]. The down-regulation of arginine biosynthetic enzymes further resulted in a decrease in the overall allocation of arginine biosynthesis, independent of oxygen availability (**Figure 20B**).

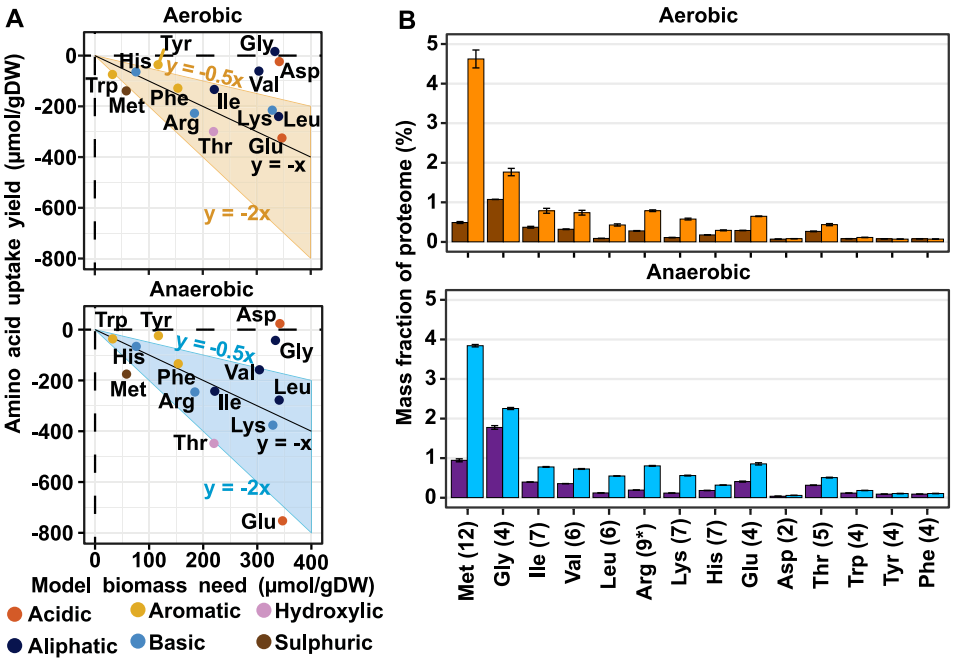

Figure 20 Amino acid supplementation allows for proteome reallocation. (A) Amino acid uptake compared to the amino acid requirement for biomass formation, as defined in the yeast consensus GEM, for both aerobic and anaerobic conditions. (B) Summarized mass proteome allocation for enzymes involved in pathways for amino acid biosynthesis (based on SGD [13]). Number in parentheses indicate the number of enzymes quantified within each pathway. ∗eight proteins were detected in samples from aerobic cultures, and nine proteins were detected in samples from anaerobic conditions. ∗p $<$ 0.05, ∗ ∗ ∗p $<$ 0.001

Similarly, for threonine, we found that the biosynthetic enzymes were down-regulated while the catabolic enzyme Gly1 [110], the major enzyme converting to threonine to glycine, was significantly up-regulated which could explain the low uptake of glycine. Again, this was coupled to a decrease in the overall proteome allocation of threonine biosynthesis, as well as a decrease in the glycine biosynthetic enzymes (**Figure 20B**). Furthermore, we observed a drastic change in the allocation of methionine biosynthetic enzymes upon supplementation of

methionine (**Figure 20B**). The summed decrease in allocation was 3 and 4% of total protein mass in aerobic and anaerobic conditions, respectively, resulting from the down-regulation of around ten enzymes in both conditions. This is in line with the highly coordinated nature of regulation of biosynthesis of sulfur-containing amino acids [111]. The large protein mass saved can be explained by the low turnover number and large molecular weight of the enzymes involved in methionine biosynthesis (data taken from the ecYeast model [43]). Interestingly, most of the protein mass saved was from a down-regulation of the last two enzymes of the pathway, with a decrease of >1% of total protein mass for both enzymes in both conditions.

In addition to the high uptake of some amino acids, we also observed a lower uptake, than required for biomass formation of the BCAAs and tyrosine. For BCAA biosynthetic enzymes, we observed a decrease in allocation adding up to a total decrease of around 1% of total proteome mass, independent of oxygen supply, but no significant increase in the BCAA catabolic enzymes.

3.1.2 Supplementation of amino acids results in reallocations in the proteome

We analyzed the data on protein abundances to identify the overall changes in proteome allocation between the different conditions. In total, we found that 9 proteins were significantly up-regulated in both aerobic and anaerobic conditions (**Figure 21A**). To characterize the gene function, we mapped the genes to gene ontology (GO)-slim terms downloaded from SGD [13]. The resulting mapping showed that four of the nine proteins were involved in catabolism of amino acids, with Car1 being the most significantly up-regulated in both conditions (log2FC 2.6 and 2.66 in aerobic and anaerobic conditions, respectively). The remaining proteins were involved in amino acid transport. We further found that 46 proteins were significantly down-regulated independent of oxygen supply (**Figure 21B**). Of these proteins, 34 were assigned GO-slim terms related to amino acid metabolic process, including many biosynthetic enzymes related to synthesis of the 14 supplemented amino acids. Furthermore, Zwf1, catalyzing the first step of the PPP, was significantly down-regulated, indicating that the flux through the PPP was lower. This could be explained by a lower requirement of NADPH and E4P, a precursor of aromatic amino acids, upon a decrease in the requirement of amino acid biosynthesis. Interestingly, we found that the summed decrease in allocation for proteins that were significantly down-regulated (given a cut-off of $|\log2FC| > 1$ and p-value < 0.05) was 10-times as large as the summed increase in allocation from proteins significantly up-regulated (6.67% down-regulated vs 0.43% of total protein mass in aerobic conditions, and 5.62% down-regulated vs 0.31% up-regulated in anaerobic conditions). This points towards a substantial down-regulation of a few proteins sustaining the up-regulation of a large number of proteins, which is in agreement with the proteome allocation model.

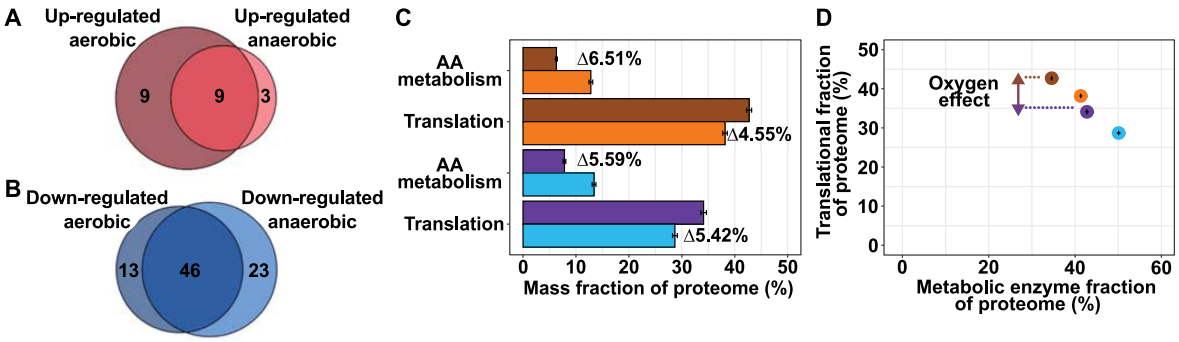

Figure 21 Supplementation of amino acids leads to a substantial remodeling of the proteome. (A)-(B) Venn diagram displaying the shared and uniquely up-regulated proteins (A) and down regulated proteins (B) comparing rich and minimal media within the two conditions. (C) Summed allocation of amino acid metabolic enzymes and translation-related proteins. The differences in allocation are highlighted between rich and minimal medium are highlighted. (D) Summed allocation of translation-related proteins vs metabolic enzyme.

3.1.3 The decrease in allocation of amino acid biosynthesis allows for an increase in translation

We next analyzed the overall changes in summed allocation of GO-slim terms and found that two groups, cellular amino acid metabolic process and cofactor metabolic process, were significantly down-regulated in both aerobic and anaerobic conditions, in line with what was seen previously. The summed allocation of the down-regulated proteins in amino acid metabolism was 6.51% in aerobic conditions and 5.59% in anaerobic conditions. Most of the terms that were significantly up-regulated were related to protein translation and the collected increase in translation was 4.55% of total protein mass in aerobic conditions and 5.42% of total protein mass in anaerobic conditions (**Figure 21C**). This shows that the majority of the cellular resources saved in amino acid metabolism are redirected toward translation to increase the overall translational capacity of the cell, which would explain the increase in growth rate seen. The general trend of biosynthetic enzymes being down-regulated and protein mass re-directed to translation was also seen for the overall metabolic fraction of the proteome (**Figure 21D**). However, although the overall trend was the same independent of oxygen supply, the allocation is different between the aerobic and anaerobic condition, potentially explained by the difference in growth rate and the fully fermentative metabolism at anaerobic conditions. The finding that increased allocation to translation allows for an increase in growth rate is in line with studies showing that there is a linear correlation between the ribosomal content and growth rate [25, 112].

3.1.4 Allocation of central carbon metabolism remains largely unchanged upon addition of amino acids

Central carbon metabolism is inherently linked to amino acid biosynthesis, since it provides the precursor metabolites required for synthesis of biomass. To evaluate the effect on central carbon metabolism from amino acid supplementation, we analyzed the allocation of proteins involved in glycolysis and the TCA cycle, which are two of the main pathways of importance to supply precursors and cofactors for amino acid biosynthesis (**Figure 22**). The main difference in terms of glycolysis was seen between anaerobic and aerobic conditions (**Figure 22A**), where the summed allocation of glycolytic proteins was almost 2-fold higher in anaerobic conditions. This could be explained by a strictly fermentative metabolism under anaerobic conditions compared to the respiro-fermentative metabolism at high growth rate aerobically [89]. The allocation of individual glycolytic enzymes was similar comparing minimal rich and minimal media between the two conditions (**Figure 22B**).

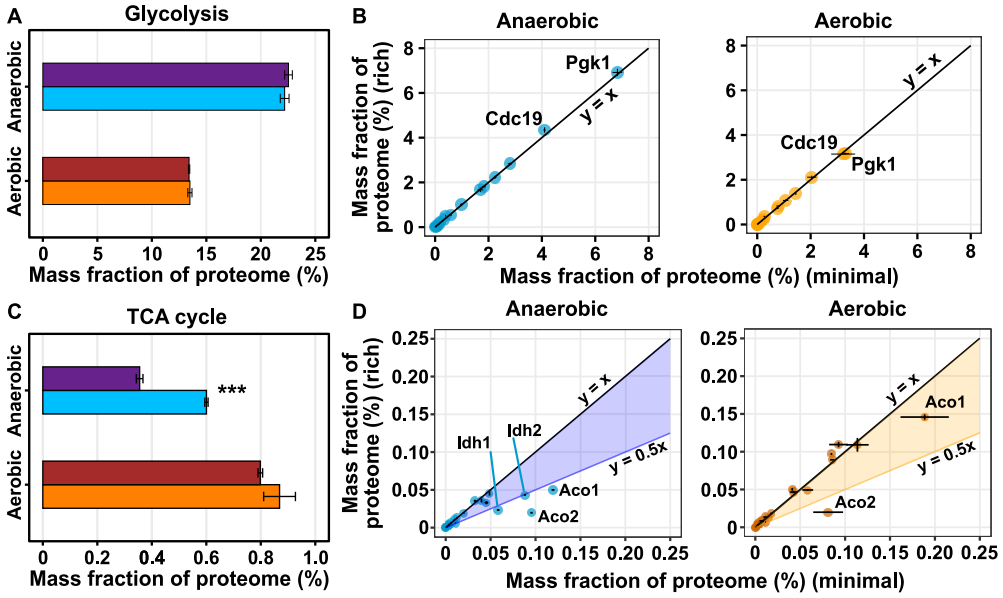

Figure 22 Most enzymes of central carbon metabolism retain their allocation when supplementing amino acids. (A) Summed allocation of glycolytic enzymes. (B) Allocation of individual glycolytic enzymes in rich vs minimal medium. (C) Summed allocation of TCA cycle enzymes. (D) Allocation of individual enzymes of the TCA cycle in rich vs minimal medium. $***p < 0.001$

For the TCA cycle, we observed a significant difference in the total allocation of proteins in anaerobic conditions, but in aerobic conditions the allocation was similar irrespective of amino acid supplementation (**Figure 22C**). During anaerobic conditions, the isocitrate dehydrogenase, consisting of subunits Idh1 and Idh2, as well as the two aconitases, Aco1 and Aco2, were down-regulated upon amino acid supplementation **Figure 22D**. Isocitrate dehydrogenase, together with Aco1 plays a key role in the initial steps of the TCA cycle converting citrate to α-ketoglutarate, an important precursor for the synthesis of glutamate and the glutamate and glutamine families of amino acids [35]. The uptake of glutamate was high in anaerobic cultures, and the observed changes are in line with reports of reduced aconitase activity upon glutamate supplementation [113]. Furthermore, the concerted down-regulation of isocitrate dehydrogenase and aconitase could imply a lower flux requirement

in the oxidative branch of the TCA cycle [114]. Interestingly, during aerobic conditions, only the two aconitases were down-regulated, although Aco1 was less significantly down-regulated while Aco2 was down-regulated 2-fold **Figure 22D**. The decrease in allocation seen in both conditions is in line with the specific role of Aco2 in biosynthesis of lysine [115], which was supplemented and taken up to an extent close to meeting the biomass requirement.

In conclusion, through the comparison of the proteome allocation in yeast grown with or without the supplementation of amino acids, both under aerobic and anaerobic conditions, we provide experimental evidence that supports the proteome allocation model for constraints on metabolism. Upon amino acid supplementation, the proteome resources saved are redirected to translation allowing for an increased translational activity allowing cells to increase their growth rate, independent on the oxygen supply. This supports previous studies proposing the use of strains with reduced proteomes as an interesting approach for increasing expression of heterologous proteins in metabolic engineering.

3.2 A comparative study of the Crabtree effect (Paper V)

Overflow metabolism in yeast, as introduced in the background section, is the strategy of using aerobic fermentation to break down glucose instead of the more efficient respiration at high glucose availability. In yeast, overflow metabolism is referred to as the Crabtree effect [27, 28]. The Crabtree effect is characterized by a high flux through glycolysis and a large fraction of the carbon being shuttled toward the fermentative pathway leading to secretion of by-products. Although the Crabtree effect has evolved independently in multiple yeast lineages, suggesting a clear competitive advantage, not all yeasts experience the Crabtree effect and some instead rely on respiration to fully oxidize glucose into carbon dioxide and water (Crabtree-negative), which in some cases can support a growth rate similar to those yeast experiencing the Crabtree effect (Crabtree-positive). Although the Crabtree effect is a well-studied phenomenon, the underlying reasons for why some Crabtree-negative yeast can reach high growth rates without any by-product formation is still not fully elucidated. According to the principles of proteome allocation, and as seen in **Paper IV**, cells must balance the allocation between energy generation and translation, making this an even more puzzling phenomenon. This has recently been explored in *S. cerevisiae* using computational approaches [116, 117]. In **Paper V** we were interested in experimentally investigating the trade-off between energy generation and growth. To do so, we performed a comparison of four yeast, two Crabtree-positive and two Crabtree-negative, to elucidate the underlying differences between the two groups. The yeasts studied were *Saccharomyces cerevisiae* and *Schizosaccharomyces pombe*, which are Crabtree-positive, as well as *Kluyveromyces marxianus* and *Scheffersomyces stipitis*, which are Crabtree-negative.

Briefly, we cultivated the four yeasts in bioreactors in minimal medium under conditions of glucose excess. An overview of the experimental setup can be seen in **Figure 23**. Since overflow metabolism has been reported in *K. marxianus* when oxygen availability is limited [118], we kept the dissolved oxygen (DO) levels above 60%. We performed a physiological

quantification, measuring the exometabolites and biomass concentration, as well performed absolute proteome quantification. We then used the data to generate condition specific models for *S. cerevisiae* and *K. marxianus*, allowing us to analyze metabolic fluxes and enzyme usage.

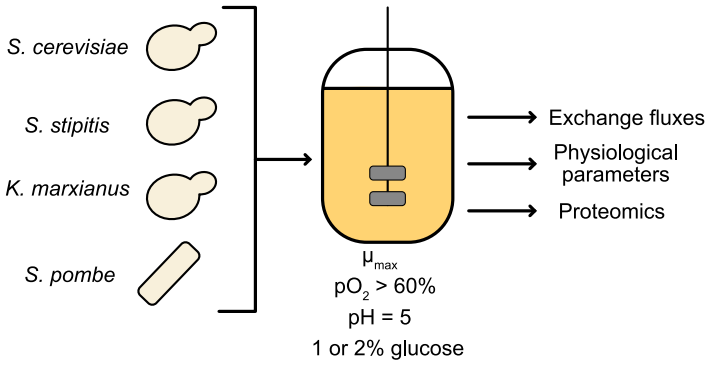

Figure 23 Overview of the experimental setup.

3.2.1 Characterization of physiological differences between Crabtree-positive and negative yeasts

To characterize the overall phenotypic differences between the Crabtree-positive and negative strains, we measured the concentration of biomass and exometabolites throughout the cultivations (**Figure 24A-D**). The Crabtree-negative yeast showed insignificant levels of by-product formation, with the exception of a small amount acetate produced by *K. marxianus*, which has also been seen in previous studies [118, 119]. The Crabtree-positive yeast produced higher levels of by-products, corresponding to >50% of the total glucose consumed for both species, in line with the occurrence of overflow metabolism. This resulted in a lower biomass yield, which was compensated for by a higher glucose uptake rate compared to the Crabtree-negative yeasts (**Figure 24F and H**). In terms of growth rate, *S. pombe* grew at around half the rate (0.22 h^{-1}) of the other three yeasts with growth rates ranging from 0.42 to 0.47 h^{-1}. Furthermore, the respiratory growth of the Crabtree-negative species was seen from the respiratory quotient (RQ) values close to 1, compared to 8.6 in the Crabtree-positive yeasts **Figure 24H**. Interestingly, the oxygen uptake rate and carbon dioxide evolution rate of *S. stipitis* was around 50% of that of *K. marxianus*. A potential explanation for this is the presence of a proton translocating NADH dehydrogenase (complex I) in the former [120] leading to an extra site of proton translocation, which in turn leads to a larger PMF and P/O ratio. This would result in a higher ATP yield per NADH oxidized, and could explain the higher biomass yield seen in *S. stipitis* compared to *K. marxianus* (**Figure 24G**).

3.2.2 The Crabtree effect is linked to differences in metabolic fluxes of central carbon metabolism and respiration

To further characterize the differences between the Crabtree-positive and negative yeast, we performed MS-based absolute proteome quantification using the iBAQ approach [59] and tandem mass tags (TMT) [121]. This resulted in the quantification of 3925, 3765, 3612 and 4110 proteins in total in *S.cerevisiae*, *S. pombe*, *K.marxianus* and *S. stipitis*, respectively.

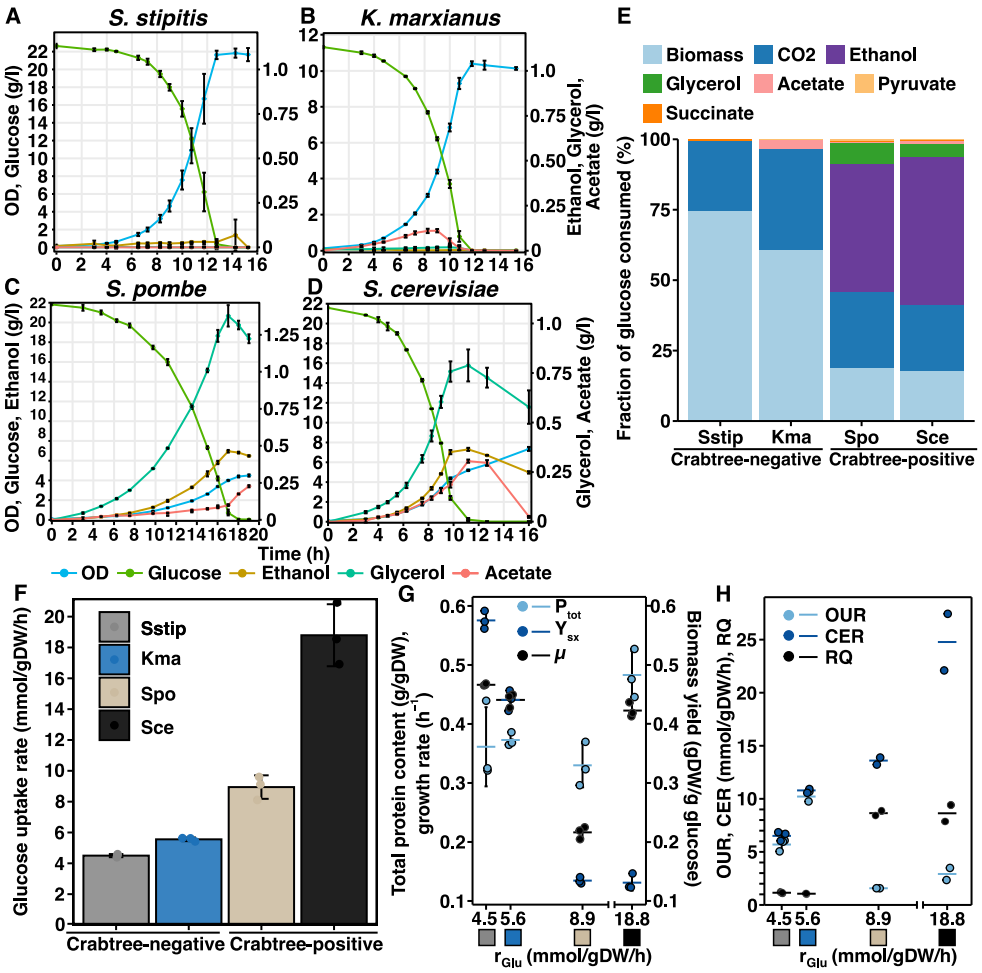

Figure 24 Physiological characterization. (A)-(D) Fermentation profiles of the four yeasts, including optical density (OD_{600}) and concentrations of glucose, ethanol, glycerol and acetate. (E) Fractional consumption of glucose (C-mmol/C-mol glucose) normalized against the total carbon recovery. (F) Glucose uptake rates. (G) Total protein content (P_{tot}), biomass yield (Y_{sx}) and growth rate (μ). (H) Oxygen uptake rate (OUR), carbon dioxide evolution rate (CER) and respiratory quotient (RQ). Mean values ± of biological triplicates are shown for all figures, except for OUR and CER, where biological duplicates were used. Sstip, *Scheffersomyces stipitis*; Kma, *Kluyveromyces marxianus*; Spo, *Schizosaccharomyces pombe*; Sce, *Saccharomyces cerevisiae*.

To investigate the metabolic adaptations underlying the Crabtree effect, we used the GECKO toolbox [43, 85] to incorporate the proteomic data and the data on exchange fluxes into the enzyme-constrained (ec) consensus yeast model and the eciSM966 *K. marxianus* model (both available from https://github.com/SysBioChalmers/ecModels). This resulted in the generation of condition-specific models constrained with the experimental data. We limited the model-based analysis to these two organisms based on the quality and standardized format of the models, facilitating the comparison of simulation results [122]. We then used the models and performed an FBA [42] simulation to obtain flux distributions. We focused the analysis on central carbon metabolism since that is where the most significant differences are expected, and compared the flux distributions of *S. cerevisiae* and *K. marxianus* (**Figure 25A**). We observed two main differences in the flux distribution, in addition to the previously discussed difference in glucose uptake rate. First, the fluxes entering the pentose phosphate pathway (PPP) at glucose-6-phosphate differed between the two yeasts. The absolute flux was higher in *S. cerevisiae*. However, the fraction of G6P metabolized in the PPP was 3-fold higher in *K. marxianus*, in line with previous studies comparing the metabolism of Crabtree-

positive and negative yeasts [123–125]. The higher absolute flux in *S. cerevisiae* could be coupled to a higher requirement of amino acid biosynthesis, which requires NADPH, due to the higher protein content (**Figure 24G**), while the lower fractional flux indicates differences in the strategy of NADPH production.

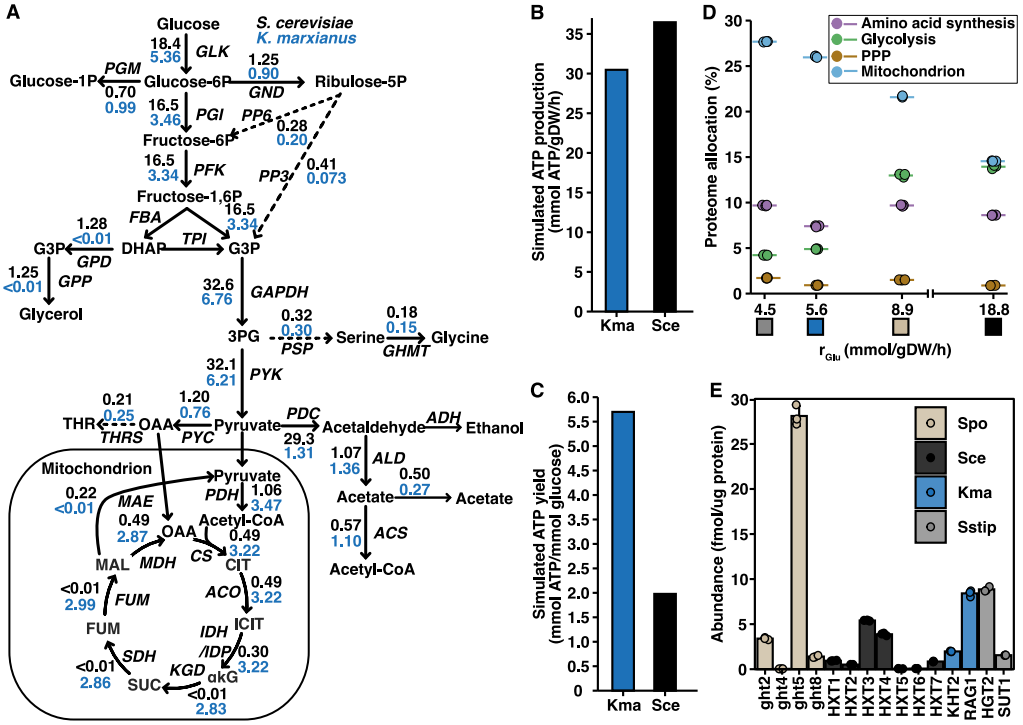

Figure 25 The trade-off between glucose utilization and ATP yield is associated to metabolic adaptations and proteome allocation. (A) Flux distribution as simulated by condition-specific models of *S. cerevisiae* and *K. marxianus*. (B)-(C) Simulated ATP production flux and yield. (D) Proteome allocation of selected processes, defined from GO terms, plotted against the glucose uptake rate. Individual values and mean values of triplicates are shown. Colored boxes indicate the organism as specified in panel E. (E) Abundances of glucose transporters. Spo, *S. pombe*; Sce, *S. cerevisiae*; Kma, *K. marxianus*; Sstip, *S. stipitis*.

The simulation results also showed a difference in fluxes around the pyruvate branching point. Along with a high flux through glycolysis, *S. cerevisiae* mainly metabolized pyruvate through pyruvate decarboxylase (PDC) and fermentation. Only a minor fraction was metabolized by pyruvate dehydrogenase and the TCA cycle, and the main flux-carrying reactions were the initial steps leading to production of α-ketoglutarate, suggesting a primary role of the cycle in providing precursor metabolites during fermentation. *K. marxianus*, on the other hand, had a lower flux through glycolysis and metabolized pyruvate mainly through the TCA cycle. Our results indicate that balancing the glycolytic flux plays an important role in the Crabtree effect. It has been shown that the PDC has a higher activity than PDH in *S. cerevisiae* [126], and would therefore be an important factor for determining the flux from pyruvate. The lower glycolytic flux in *K. marxianus* could therefore be a strategy for ensuring that the PDH activity is sufficient to support fully respiratory catabolism of pyruvate.

The differences in fluxes were reflected by the simulated ATP production. The net ATP production flux, combining the ATP production of glycolysis and respiration, equal to the ATP consumption of the cell, was slightly lower in *K. marxianus* (**Figure 25B**), indicating a more efficient ATP utilization for biomass. Furthermore, *K. marxianus* showed a 3-fold

higher ATP yield (**Figure 25C**). These results highlight the differences in strategies in energy generation, where *K. marxianus* balances the flux through glycolysis to maintain a high efficiency of ATP production, while *S. cerevisiae* compensates for the low efficiency of fermentation by a high glycolytic flux.

3.2.3 Proteome allocation reflects the trade-off between glucose strategies for glucose utilization and ATP yield

We summed the allocation of individual proteins based on GO term annotation [127] and compared the differences in allocation of selected processes (**Figure 25D**). In line with the results of the model-based analysis, the Crabtree-positive species showed a higher allocation of proteins to glycolysis at the expense of mitochondrial proteins, reflecting the fermentative strategy of glucose utilization. However, only small differences were observed for amino acid biosynthesis and the PPP, indicating that the main distinguishing factor between the groups is in energy metabolism.

A major event in the evolution of *S. cerevisiae* was the increase in glycolytic gene dosage following a whole-genome duplication [128, 129] and it has been suggested to be an important factor in the evolution of the Crabtree effect. When analyzing the levels of glycolytic proteins, we indeed found that the Crabtree-positive species showed higher levels of all proteins. Although *S. pombe* has not gone through a WGD, some glycolytic genes are duplicated [130], and we found that the single copy enzymes showed similar abundance as the summed abundance of the *S. cerevisiae* orthologs. Additionally, we found differences in the number and abundance of active glucose transporters (**Figure 25E**) both between the two Crabtree-positive yeasts and between the groups of yeasts. The Crabtree-negative yeasts as well as *S. pombe*, based on abundance, seemed to rely mainly on a single transporter while *S. cerevisiae* distributed the expression among several transporters. Glucose transport has been proposed to be one of the key flux-controlling steps of glycolysis [129, 131, 132], and our result suggest that the optimization of glucose transporters for rapid glucose uptake is an important factor in the Crabtree effect.

3.2.4 Limitations in the electron transport chain and ATP synthase are characteristic for the Crabtree effect

We calculated the capacity usage, defined as the ratio between enzyme demand predicted in ec-model simulations and the measured enzyme levels, for energy related processes in *S. cerevisiae* and *K. marxianus* (**Figure 26A**). Here, we found that *S. cerevisiae* had a higher usage of enzymes involved in glycolysis and PPP, while *K. marxianus* had a higher usage in the TCA cycle. These findings indicate that the flux differences of these pathways are not only coupled to increases in expression but also to a higher usage of the enzymes. The usage of proteins in the ETC and ATP synthase was close to 100% in both species, indicating that the cells balance the expression of these proteins based on the demand. This makes sense from a biological standpoint since they are membrane-bound meaning that any unused proteins would occupy membrane space and therefore compete with other membrane proteins such as carrier proteins.

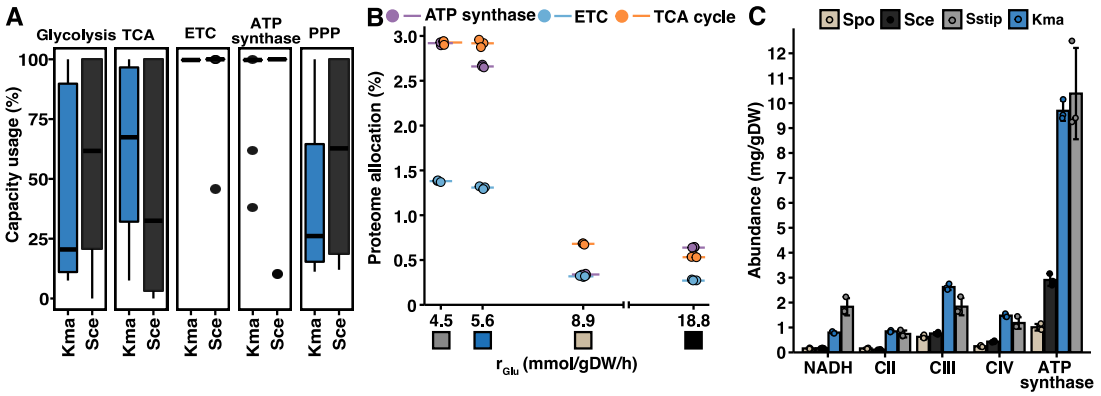

Figure 26 The Crabtree effect is characterized by limitations in the ETC and ATP synthase. (A) Capacity usage of energy-related process in *S. cerevisiae* and *K. marxianus*, calculated as the ratio between model predicted enzyme demand and the experimentally measured enzyme levels. (B) Allocation of ATP synthase, ETC and TCA cycle. (C) Abundances of ATP synthase and individual complexes of the ETC. NADH, NADH dehydrogenases; CII, complex II; CIII, complex III; CIV, complex IV.

We next analyzed the allocation of the processes in the four yeasts. The two Crabtree negative yeasts, showed a more than 3-fold higher allocation of the TCA cycle, ETC and ATP synthase, which was also reflected in the abundance of the individual complexes of the ETC and ATP synthase (**Figure 26B and C**). These results, together with the trend of increasing allocation of glycolytic proteins at expense of respiration (**Figure 25D**) in the Crabtree-positive yeasts point towards the high glycolytic flux causing a saturation of the capacity of NADH reoxidation in respiration leading to increased fermentation. Limitations in the capacity of NADH re-oxidation have previously been suggested as one of the drivers of overflow metabolism in *S. cerevisiae* [133].

3.2.5 The Crabtree effect is accompanied by differences in translation

The evolutionary advantage of the Crabtree effect is thought to be that it allows for a higher rate of ATP production, therefore allowing Crabtree-positive yeasts to grow at a higher rate in glucose excess conditions [89]. However, our data shows that *S. cerevisiae* and the Crabtree-negative yeasts grow at similar rates, and that *S. pombe*, although being Crabtree-positive, grows at about half the rate (**Figure 24G**). This point towards some other constraint that limits the growth rate. A natural candidate for such a constraint is protein translation. The WGD in *S. cerevisiae* resulted in the retention of 59 of 78 ribosomal proteins (RPs) in duplicates [134], in addition to duplication of genes in carbohydrate metabolism. Interestingly, although the Crabtree-effect evolved independently in *S. pombe*, 62 of 78 RPs have paralogs. The Crabtree-negative yeasts, however, have no RP paralogs. The evolution and retention of RP paralogs, could contribute to a specialization of ribosomes, potentially with slower kinetics as a consequence. This led us to analyze the ribosomal content and translation efficiency.

Our data shows that the ribosomal content was 19.5-23.6% of total protein mass in the faster growing yeasts (*S. cerevisiae, K. marxianus* and *S. stipitis*) and 16.1% in *S. pombe*. This agrees with previous studies reporting a linear increase in RP abundance with increasing

growth rate [25, 112]. We calculated the translation efficiency and found that *S. stipitis* had the highest efficiency, *S. cerevisiae* and *K. marxianus* had similar efficiencies, while *S. pombe* had the least efficient translation (**Figure 27A**). Given the differences seen in the expression of ETC components and ATP synthase (**Figure 26**), we also examined the abundance and translation efficiency of the mitochondrial ribosomes, responsible for translating some key subunits of the complexes. Here, we found that the mitochondrial ribosomal content of the Crabtree-positive yeast was only 28% of that of the Crabtree-negative yeasts (Figure 27B). We calculated the efficiency of the mitochondrial ribosomes using mean subunit abundance of the ETC complexes and ATP synthase as a proxy for the mitochondrially synthesized proteins. We again found that *S. cerevisiae* and *K. marxianus* had similar efficiencies, while *S stipitis* had the highest efficiency and *S. pombe* the lowest (**Figure 27C**). The less efficient cytosolic ribosomes together with the lower expression of mitochondrial ribosomes, and differences in efficiency of mitochondrial ribosomes could explain the much lower levels of expression seen for cytochrome c oxidase and ATP synthase seen in the Crabtree-positive species (**Figure 27D**), although further studies including more yeast species would be required to confirm this observation.

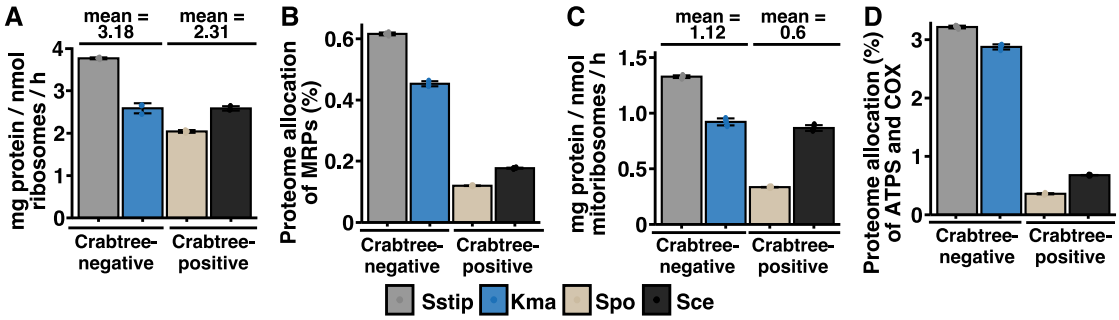

Figure 27 The Crabtree effect is associated to differences in translation. (A) Overall translation efficiency. (B) Allocation of mitochondrial ribosomal proteins (MRPs), calculated as percent of total protein. (C) Translation efficiency of mitochondrial ribosomes. (D) Allocation of ATP synthase (ATPS) and cytochrome c oxidase (COX). Sstip, *S. stipitis*; Kma, *K. marxianus*; Spo, *S. pombe*; Sce, *S. cerevisiae*

Taken together, this study shows that the Crabtree effect in yeast is coupled to adaptations in both central carbon metabolism and protein translation, related to differences in the strategy of ATP production. We, to the best of our knowledge, performed the first quantitative comparison of Crabtree-positive and negative yeasts on the proteome level. In addition to the insights obtained on the underlying causes of the Crabtree effect, we provide a dataset of absolute protein abundances that could serve as a valuable resource for further studies on this important phenomenon.

Conclusions and perspectives

The work presented in this thesis has revolved around using systems biology approaches to study the metabolism of yeast, mainly *Saccharomyces cerevisiae*, with the overall aim of increasing the understanding of the metabolism and physiology of this model eukaryon. The approaches have consisted of proteomic analysis, constraint-based modeling and general physiological characterization of yeast and mitochondria harvested from a diverse set of conditions.

4.1 Part I: Investigating mitochondrial metabolism

In part I, I presented two studies on mitochondrial metabolism, which is not only important for energy generation, but also contributes to the synthesis of important metabolites such as amino acids and cofactors, as reviewed in **Paper I**. In **Paper II**, we performed a thorough analysis of mitochondrial metabolism during the different stages of a batch cultivation. We presented a novel approach for quantifying the mitochondrial proteome on a subcellular level, building upon the combination of quantification of biophysical parameters and microscopy imaging to determine the mitochondrial volume. Through this approach, we were able to identify the transition of mitochondria from being a biosynthetic hub providing cellular building blocks at fast growth to a center for energy generation during respiration. Furthermore, we identified the diauxic shift as a phase where major structural and metabolic changes on the mitochondrial level occur. We found that as glucose is exhausted, there is a drastic up-regulation in response to the shift towards respiratory metabolism, involving the TCA cycle, respiratory chain, ATP synthase as well as mitochondrial carriers. Our findings indicated that these processes are part of an early response to glucose exhaustion that lasts throughout the diauxic shift, in line with what was observed in a previous study on the temporal dynamics of the yeast proteome during the diauxic shift [54]. In addition to these processes, we found an enrichment of proteins involved in mitochondrial gene expression and translation, mitochondrial organization, protein import, and respiratory chain complex assembly among proteins specifically up-regulated in the diauxic shift. This highlights the importance of mitochondrial biogenesis at an early stage of the transition from fermentation to respiration. These processes were not found by Murphy et al. [54]. We hypothesize that studies quantifying the overall cellular proteome, including our analysis of the cellular proteome, fail to capture these changes specifically occurring at the mitochondrial level due to not accounting for the increase in mitochondrial mass as cells go through the diauxic shift. Many of these changes are less abundant and would therefore be more difficult to capture without specifically targeting the mitochondrial proteome.

During recent years, the mitochondrial proteome has been given increasing attention owing to the central role of mitochondria in cellular function. Many studies have focused on

defining the mitochondrial proteome in terms of the entire set of proteins, their function and localization as well as the protein levels and dynamics [46, 47, 74, 135, 136]. Our study contributes to the knowledge on the mitochondrial proteome by extending the number of proteins identified in mitochondria as well as providing insight into the dynamics of the mitochondrial proteome. As we showed, focusing on isolated mitochondria allows the detection of more subtle changes in the mitochondrial proteome that may otherwise go undetected. Unfortunately, studying the dynamics of mitochondria is to some extent limited by the low throughput of mitochondrial isolation. As faster techniques for isolation of mitochondria become available, studies expanding our work to include multiple timepoints in the diauxic shift to capture the dynamics in more detail would be very interesting.

In **Paper III** I, for the first time, constructed a genome-scale model describing mitochondrial protein translocation in an eukaryal organism. The model also included a detailed description of the proton motive force, as well as the synthesis and incorporation of cofactors synthesized partially or entirely in mitochondria, including Fe-S clusters, lipoic acid, and heme. Fe-S cluster biosynthesis and mitochondrial protein import are essential for cell viability in any given condition [36, 90] and are therefore imperative for a comprehensive model of mitochondrial metabolism. Interestingly, although the activity of the mitochondria varies significantly depending on the mode of metabolism, the levels of the mitochondrial protein import and the Fe-S biosynthetic machinery remains a rather constant part of the mitochondrial proteome (**Paper II**). We used the model to investigate the dynamics of mitochondrial protein import and Fe-S biosynthesis, as well as to estimate the energy cost of metabolite transport across the mitochondrial inner membrane. We found that for protein import, the model predicts a dynamic behavior where the requirement of protein import machineries scale with respiratory activity, in good agreement with experimental observations. For the Fe-S biosynthetic machinery on the other hand, model predictions showed a worse correlation with experimental data, with an underprediction of the protein requirements. This could indicate that the cells keep a reserve capacity of these proteins in order to ensure that no potentially toxic intermediates in the Fe-S cluster synthesis are released but also that the parameters used in the model need to be further curated.

The model represents a knowledge base for reactions in protein import and Fe-S biosynthesis. Although there is a vast amount of literature on the processes described, the data on mechanistic details are still scarce. As any protein-constrained GEM, the model relies on the protein turnover numbers (k_{cat}) of enzymes. These two factors have implications for the model performance as the simulation performance depends on the k_{cat} values chosen [137]. Therefore, improvements of model predictions are likely to come from further characterization of the k_{cat} values of, in particular protein import and Fe-S cluster biosynthesis, but also from an overall increase in the coverage of metabolic enzymes and transporters in *S. cerevisiae*. This could come from further experimental studies or computational approaches that have been shown to perform well in predicting turnover numbers based on fluxes and proteomics data [138]. Additionally, the model is based on the current knowledge and the scope is limited to metabolic enzymes. However, the framework used to develop ecMitoYeast can easily be

updated to represent newly discovered metabolic content and the related enzymes. Increasing the scope to modeling metabolism and gene expression, using a so-called ME model, as successfully done to model protein translocation in *E. coli* [139], would improve the predictions by substantially increasing the coverage. Two ME models have recently been developed for *S. cerevisiae* [140, 141], opening up an exciting avenue for future modeling-driven studies of mitochondrial metabolism. As the accuracy of the models increase, their use in integration and analysis of omics data, such as proteomics, will be a valuable tool for future studies.

I envision that ecMitoYeast could serve as a valuable complement to experimental studies. The processes reconstructed here, can also partly be integrated into the metabolic and enzyme-constrained yeast consensus model [84] and contribute to further expansions both in the scope and accuracy of those models. Additionally, an accurate representation of mitochondrial protein import would be imperative in the further development of the yeast ME-models in the future endeavor of creating a model describing the yeast cell as a whole. Lastly, given the high conservation of mitochondrial protein import as well as Fe-S cluster biosynthesis, and the recent developments in modeling human metabolism [142], the framework used to develop ecMitoYeast could be adapted to allow the reconstruction of these processes in human cells. Such a model would allow for studying mitochondrial function and dysfunction in relation to mitochondrial diseases directly in Human.

4.2 Part II: Investigating constraints in cellular metabolism

In part II of this thesis, I presented two studies focusing on investigating the constraints in cellular metabolism that give rise to specific phenotypes. In **Paper IV**, we investigated the effect of supplementing amino acids on the physiology and proteome allocation of *S. cerevisiae* by cultivating the yeast with or without supplementation of amino acids in both aerobic and aerobic conditions, and quantifying the concentration of medium components and abundances of proteins. We found that as the burden of biosynthesis of amino acids is relieved, the cells reallocate proteome resources to protein translation, which resulted in an increased growth rate and biomass yield. The principles of proteome allocation in yeast have previously been explored using computational approaches [116], and a few studies have investigated proteome allocation experimentally [25, 143]. Our study provides experimental evidence for the proteome allocation theory [103], and highlight the importance of balancing the allocation of proteome resources as well as how the trade-offs between allocation to protein translation and other cellular processes give rise to constraints on cellular growth rate.

Translation capacity is thought to be one of the main factors limiting growth [144]. This has been seen both in studies overexpressing a non-essential protein to increase the burden of proteins synthesis of the cell [103, 145], and studies using gene deletions to reduce the requirements for synthesis of proteins other than those necessary for cellular proliferation, in both *E. coli* and yeast. As an example, D'Souza et al. (2014) [146] deleted genes in pathways for synthesis of single amino acids, nucleotides or vitamins in *E. coli*, and showed that when supplementing the resulting auxotrophy, the maximum specific growth rate was increased. They further saw that the beneficial effect on growth was larger the higher the

protein expression of the genes deleted were, supporting that protein translation capacity is an important constraint on the growth rate of cells. Similarly, our results add further experimental evidence to this, in yeast, by showing that removing the need for synthesis of 14 amino acids results in a substantial amount of protein mass being freed up and used by cells to increase their translational capacity and grow faster. Further studies into the effects of supplementing biomass precursors would be interesting to see how much the growth rate of cells can be increased. Although I would expect that there is some room for further increases in growth rate, as seen by the higher growth rates of yeast in rich YPD medium, at some point the cell is going to hit another constraint on growth that cannot be overcome by simply allocating more proteome mass to translation. For investigating this constraint, I think that the recent development of ME-models mentioned above could play an important role in complementing experimental research, not only in verifying the hypothesis generated in our study but to perform further *in silico* experiments on proteome allocation. These models allow the investigation of the effect of perturbations, such as nutrient supplementation, on the expression levels of proteins and the machinery required for protein synthesis. The potential of these models for investigating constraints on cellular metabolism arising from the finite protein resources has already been demonstrated in *E. coli* [147]. It has been proposed from studies in *E. coli* that the cell growth rate is ultimately limited by the rate of synthesis of ribosomes [148–150]. These studies have involved extensive investigation of the biophysical limits of the cells, mechanistic modeling of ribosomes, as well as proteomics data-driven analysis, highlighting the interdisciplinarity of systems biology and the value of both top-down and bottom-up systems biology. These studies argue that while many processes can be sped up by increasing protein abundances or increasing DNA replication, this is not the case for synthesis of ribosomes. As a consequence, the translation time for each ribosome places an inherent limit on the growth rate that can only be overcome by increasing the protein elongation rate or altering the composition of the ribosome. It would be interesting to see if systems biology studies in yeast, utilizing the increasing amount of proteomics data and mechanistic insights, would reach the same conclusions and if these findings can be extended also to eukaryal cells.

An exciting application of the findings on proteome reallocation would be in the construction of lean proteome strains in metabolic engineering, as proposed by Valgepea et al. (2015) [151]. An important challenge in metabolic engineering is that the expression of heterologous proteins required for synthesis of the desired product competes with the expression of the native proteins adding an additional protein cost, often-times resulting in a reduction of the growth rate [145]. By deleting genes encoding non-essential proteins, the cellular protein synthesis requirement would be reduced, with an increasing fraction of the proteome being freed up for proteins synthesis, potentially increasing the production of the heterologous proteins required for synthesis of a desired product with increased production as a consequence. A main challenge in this approach is to identify the targets for deletion. When it comes to yeast, I believe that the increasing abundance of proteomics datasets from a diverse set of conditions, the existence of a gene deletion collection [14], as well as the emergence of ME-models [140, 141], could aid in elucidating targets with a non-inhibitory effect on growth

that at the same time represent a large enough fraction of the proteome to see a beneficial effect.

In **Paper V**, we quantitatively described the metabolic and proteomic adaptations underlying the Crabtree effect by comparing the Crabtree-positive yeasts *S. cerevisiae* and *S. pombe* to the Crabtree-negative yeasts *K. marxianus* and *S. stipitis*, cultivated in glucose excess conditions. We used an approach combining physiological and proteome quantification and genome-scale metabolic modeling and found that the Crabtree effect is associated to adaptations in metabolism and protein translation reflecting the trade-off between glucose utilization strategies in terms of the rate and yield of ATP production. Optimal carbon usage is crucial to synthesize the ATP and biomass precursors required for cell growth. We found that the Crabtree-positive yeasts utilize a strategy to maximize the rate of ATP production using glycolysis and fermentative pathways, and balance the low ATP yield of the pathway by a high glucose uptake. Contrastingly, the Crabtree-negative yeasts balance the glucose uptake to maintain sufficient capacity of the respiratory pathway to fully oxidize glucose, resulting in a high ATP yield. The two approaches differ in the protein cost, where fermentation is less efficient but less costly in terms of protein mass, and respiration is more efficient but requires more protein mass. Our data on proteome allocation showed that the total proteome mass allocated to energy metabolism, consisting of glycolysis, the TCA cycle, ETC and ATP synthase, was roughly the same among the four yeasts. This suggests that there is a limit to the maximum proteome fraction allocated to energy metabolism, acting as an additional constraint on the growth rate. This is in line with a recent modeling-based study showing that increasing the proteome fraction of energy metabolism is a potential mechanism to increase the growth rate [117]. Furthermore, we found a lower content and translational efficiency of both cytosolic and mitochondrial ribosomes in *S. pombe* compared to the Crabtree-negative yeasts, suggesting that differences in translation is an underlying cause of the Crabtree effect. This is an intriguing finding given that a major event in the evolution of both *S. cerevisiae* and *S. pombe* was the duplication of ribosomal genes, and future studies expanding on our work to include additional yeast species would be highly interesting to confirm the findings of our study.

In summary, the research performed in this thesis highlights the value of using a systems biology approach to study metabolism. It shows that the combination of experimental studies with constraint-based modeling is a powerful strategy for gaining insights into the various aspects related to metabolism, ranging from mitochondrial metabolism to the overall proteome allocation and the imposed constraints evaluated in this thesis. I believe that the frameworks presented here, together with the datasets and model generated, will provide value in generating and testing hypotheses in future studies.

Acknowledgements

During my PhD studies I have had the pleasure of meeting a lot of great people and have gotten a fantastic support from the people around me. Therefore, I would like to start by thanking each and every person that has been part of this journey, without whom this thesis never would have existed.

Thanks to my supervisor, Jens, for providing me with the opportunity to be part of the SysBio community, for letting me work on interesting projects and for your continuous support and encouragement throughout my studies. You have been a great mentor to me and I have always left our meetings with a smile, excited about my research projects. Thanks to my two co-supervisors. Ed for your guidance, helpful suggestions and thorough reviews of my manuscripts. Christer for your valuable input and for providing me with the opportunity to teach in one of your courses.

The work in this thesis would not have been possible without the help of my collaborators. Thanks to Francesca for teaming up with me to work on mitochondria, for all our interesting discussions and all the fun we had during our never-ending fermentations. Thanks to Johan for our valuable discussions and interesting projects, but also for being a friend and a great support throughout most of my time at Chalmers. Thanks also to Rosemary and Kate for your valuable input. Finally, thanks to Gang for our interesting discussions and your company as an office mate.

Being part of the SysBio family during my PhD studies has been a truly inspiring experience. Thanks to all current and former members of SysBio for creating such a great atmosphere to work in. I think our core values describe the people at SysBio very well. Even though you are all hard-working people with a lot on your plate, there was always room for discussion and for lending a helping hand when needed. I will cherish the many happy memories created during my time at SysBio.

I would like to end by thanking my family. Mom and dad for always being there to support me and for always believing in me even at times when I did not. Lucas, you have been there from my very first moment in life and we have shared so many memories together. Thank you for always cheering me up and being there whenever I need you. Tack till mormor, morfar, och farmor. Ni är och har varit en stor inspiration för mig. Tack för alla fina stunder genom åren. Last but not least, thanks to Gabriella for your endless love and support through my many ups and downs and for inspiring me to be the best person I can be. Without you this never would have been possible. I cannot describe how much all of you mean to me.

References

1. Scrödinger, E. *What is life?: the physical aspect of the living cell* (Cambridge Univ. Press, 1944).
2. Westerhoff, H. V. & Palsson, B. O. The evolution of molecular biology into systems biology. *Nat Biotechnol.* **22,** 1249–52 (2004).
3. Kitano, H. Systems Biology : A Brief Overview. *Science* **295,** 1662–1665 (2002).
4. Vidal, M. A unifying view of 21st century systems biology. *FEBS Lett.* **583,** 3891–3894 (2009).
5. Breitling, R. What is systems biology ? *Front. Physiol.* **1,** 1–5 (2010).
6. Bruggeman, F. J. & Westerhoff, H. V. The nature of systems biology. *TRENDS Microbiol.* **15,** 45–50 (2006).
7. Nielsen, J. Systems Biology of Metabolism. *Annu. Rev. Biochem.* **86,** 1–35 (2017).
8. Kell, D. B. & Oliver, S. G. Here is the evidence , now what is the hypothesis ? The complementary roles of inductive and hypothesis-driven science in the post-genomic era. *BioEssays* **26,** 99–105 (2004).
9. Smallbone, K., Messiha, H. L., Carroll, K. M., *et al.* A model of yeast glycolysis based on a consistent kinetic characterisation of all its enzymes. *FEBS Lett.* **587,** 2832–2841 (2013).
10. Botstein, D., Chervitz, S. A., Cherry, J. M., *et al.* Yeast as a Model Organism. *Science* **277,** 1259–1260 (1997).
11. Oliver, S. G., van der Aart, Q. J. M., Agostoni-Carbone, M. L., *et al.* The complete DNA sequence of yeast chromosome III. *Nature* **357,** 38–46 (1992).
12. Goffeau, A., Barrell, B. G., Bussey, H., *et al.* Life with 6000 Genes. *Science* **274,** 546–567 (1996).
13. Cherry, J. M., Hong, E. L., Amundsen, C., *et al.* Saccharomyces Genome Database: the genomics resource of budding yeast. *Nucleic Acids Res.* **40,** D700–D705 (2012).
14. Giaever, G. & Nislow, C. The Yeast Deletion Collection: A Decade of Functional Genomics. *Genetics* **197,** 451–465 (2014).
15. Nielsen, J., Larsson, C., Maris, A. V. & Pronk, J. Metabolic engineering of yeast for production of fuels and chemicals. *Curr. Opin. Biotechnol.* **24,** 398–404 (2013).
16. Krivoruchko, A. & Nielsen, J. Production of natural products through metabolic engineering of Saccharomyces cerevisiae. *Curr. Opin. Biotechnol.* **35,** 7–15 (2015).

17. Wood, V., Gwilliam, R., Rajandream, M., *et al.* The genome sequence of Schizosaccharomyces pombe. *Nature* **415,** 871–880 (2002).

18. Yanagida, M. The model unicellular eukaryote, Schizosaccharomyces pombe. *Genome Biol.* **3,** 1–4 (2002).

19. Lane, M. M. & Morrissey, J. P. Kluyveromyces marxianus : A yeast emerging from its sister's shadow. *Fungal Biol. Rev.* **24,** 17–26 (2010).

20. Jeffries, T. W. Engineering yeasts for xylose metabolism. *Curr. Opin. Biotechnol.* **17,** 320–326 (2006).

21. Stephanopoulos, G. N., Aristidou, A. A. & Nielsen, J. in *Metabolic engineering: principles and methodologies* Chapter 3, 21–79 (Academic Press, San Diego, 1998).

22. Kuhn, K. M., Risi, J. L. D. E. & Brown, P. O. Global and Specific Translational Regulation in the Genomic Response of Saccharomyces cerevisiae to a Rapid Transfer from a Fermentable to a Nonfermentable Carbon Source. *Mol. Cell. Biol.* **21,** 916–927 (2001).

23. Godard, P., Urrestarazu, A., Kontos, K., *et al.* Effect of 21 Different Nitrogen Sources on Global Gene Expression in the Yeast Saccharomyces cerevisiae. *Mol. Cell. Biol.* **27,** 3065–3086 (2007).

24. Paulo, J. A., O'Connell, J. D., Everley, R. A., *et al.* Quantitative mass spectrometry-based multiplexing compares the abundance of 5000 S. cerevisiae proteins across 10 carbon sources. *J. Proteomics* **148,** 85–93 (2016).

25. Metzl-Raz, E., Kafri, M., Yaakov, G., *et al.* Principles of cellular resource allocation revealed by condition-dependent proteome profiling. *eLife* **6,** 1–21 (2017).

26. Molenaar, D., Berlo, R. V. & de Ridder, D. Shifts in growth strategies reflect tradeoffs in cellular economics. *Mol. Syst. Biol.* **5,** 1–10 (2009).

27. Crabtree, H. G. OBSERVATIONS ON THE CARBOHYDRATE METABOLISM OF TUMOURS. *Biochem. J.* **23,** 536–545 (1929).

28. De Deken, R. H. The Crabtree Effect : A Regulatory System in Yeast. *J. Gen. Microbiol.* **44,** 149–156 (1966).

29. Gray, M. W., Burger, G. & Lang, B. F. Mitochondrial Evolution. *Science* **283,** 1476–1481 (1999).

30. Cavalier-Smith, T. The Origin of Eukaryote and Archaebacterial Cells. *Ann. N. Y. Acad. Sci.* **503,** 17–54 (1987).

31. Cox, C. J., Foster, P. G., Hirt, R. P., *et al.* The archaebacterial origin of eukaryotes. *Proc Natl Acad Sci U S A* **105,** 20356–20361 (2008).

32. Lane, N. & Martin, W. The energetics of genome complexity. *Nature* **467,** 929–34 (2010).

33. Westermann, B. Bioenergetic role of mitochondrial fusion and fission. *Biochim. Biophys. Acta* **1817,** 1833–1838 (2012).

34. Palmieri, F. & Pierri, C. L. Mitochondrial metabolite transport. *Essays Biochem.* **47,** 37–52 (2010).

35. Ljungdahl, P. O. & Daignan-Fornier, B. Regulation of amino acid, nucleotide, and phosphate metabolism in Saccharomyces cerevisiae. *Genetics* **190,** 885–929 (2012).

36. Lill, R. & Freibert, S. Mechanisms of Mitochondrial Iron-Sulfur Protein Biogenesis. *Annu. Rev. Biochem.* **89,** 471–499 (2020).

37. Horvath, S. E. & Daum, G. Lipids of mitochondria. *Prog. Lipid Res.* **52,** 590–614 (2013).

38. Xu, Y., Anjaneyulu, M., Donelian, A., *et al.* Assembly of the complexes of oxidative phosphorylation triggers the remodeling of cardiolipin. *Proc. Natl. Acad. Sci. U S A* **116,** 11235–11240 (2019).

39. Hiltunen, J. K., Schonauer, M. S., Autio, K. J., *et al.* Mitochondrial Fatty Acid Synthesis Type II: More than Just Fatty Acids. *J. Biol. Chem.* **284,** 9011–9015 (2009).

40. Almquist, J., Cvijovic, M., Hatzimanikatis, V., Nielsen, J. & Jirstrand, M. Kinetic models in industrial biotechnology - Improving cell factory performance. *Metab. Eng.* **24,** 38–60 (2014).

41. Bordbar, A., Monk, J. M., King, Z. A. & Palsson, B. O. Constraint-based models predict metabolic and associated cellular functions. *Nat. Rev. Genet.* **15,** 107–120 (2014).

42. Orth, J. D., Thiele, I. & Palsson, B. Ø. What is flux balance analysis? *Nat. Biotechnol.* **28,** 245–248 (2010).

43. Sánchez, B. J., Zhang, C., Nilsson, A., *et al.* Improving the phenotype predictions of a yeast genome-scale metabolic model by incorporating enzymatic constraints. *Mol. Syst. Biol.* **13,** 1–16 (2017).

44. Aebersold, R. & Mann, M. Mass spectrometry-based proteomics. *Nature* **422,** 198–207 (2003).

45. Cox, J. & Mann, M. Quantitative, high-resolution proteomics for data-driven systems biology. *Annu. Rev. Biochem.* **80,** 273–299 (2011).

46. Morgenstern, M., Stiller, S. B., Lübbert, P., *et al.* Definition of a High-Confidence Mitochondrial Proteome at Quantitative Scale. *Cell Rep.* **19,** 2836–2852 (2017).

47. Vögtle, F.-N., Burkhart, J. M., Gonczarowska-Jorge, H., *et al.* Landscape of submitochondrial protein distribution. *Nat. Commun.* **8,** 290 (2017).

48. Gorman, G. S., Chinnery, P. F., DiMAuro, S., *et al.* Mitochondrial Diseases. *Nat Rev Dis Primers* **2,** 16080 (2016).

49. Gancedo, J. M. Carbon catabolite repression in yeast. *Eur. J. Biochem.* **206,** 297–313 (1998).

50. Kayikci, Ö. & Nielsen, J. Glucose repression in Saccharomyces cerevisiae. *FEMS Yeast Res.* **15,** 1–8 (2015).

51. Brauer, M. J., Saldanha, A. J., Dolinski, K. & Botstein, D. Homeostatic Adjustment and Metabolic Remodeling in Glucose-limited Yeast Cultures. *Mol Biol Cell* **16,** 2503–2517 (2005).

52. Zampar, G. G., Kümmel, A., Ewald, J., *et al.* Temporal system-level organization of the switch from glycolytic to gluconeogenic operation in yeast. *Mol. Syst. Biol.* **9,** 651 (2013).

53. Galdieri, L., Mehrotra, S., Yu, S. & Vancura, A. Transcriptional regulation in yeast during diauxic shift and stationary phase. *OMICS* **14,** 629–638 (2010).

54. Murphy, J. P., Stepanova, E., Everley, R. A., Paulo, J. A. & Gygi, S. P. Comprehensive Temporal Protein Dynamics during the Diauxic Shift in Saccharomyces cerevisiae. *Mol. Cell. Proteomics* **14,** 2454–2465 (2015).

55. Renvoisé, M., Bonhomme, L., Davanture, M., *et al.* Quantitative variations of the mitochondrial proteome and phosphoproteome during fermentative and respiratory growth in Saccharomyces cerevisiae. *J. Proteomics* **106,** 140–150 (2014).

56. Ohlmeier, S., Kastaniotis, A. J., Hiltunen, J. K. & Bergmann, U. The Yeast Mitochondrial Proteome, a Study of Fermentative and Respiratory Growth. *J. Biol. Chem.* **279,** 3956–3979 (2004).

57. Martin, J., Mahlke, K. & Pfanner, N. Role of an energized inner membrane in mitochondrial protein import: $\Delta\Psi$ drives the movement of presequences. *J. Biol. Chem.* **266,** 18051–18057 (1991).

58. Meisinger, C., Pfanner, N. & Truscott, K. N. Isolation of yeast mitochondria. *Methods Mol. Biol.* **313,** 33–39 (2006).

59. Schwanhäusser, B., Busse, D., Li, N., *et al.* Global quantification of mammalian gene expression control. *Nature* **473,** 337–342 (2011).

60. Egner, A., Jakobs, S. & Hell, S. W. Fast 100-nm resolution three-dimensional microscope reveals structural plasticity of mitochondria in live yeast. *Proc. Natl. Acad. Sci. U S A* **99,** 3370–3375 (2002).

61. Rafelski, S. M., Viana, M. P., Zhang, Y., *et al.* Mitochondrial Network Size Scaling in Budding Yeast. *Science* **338,** 822–824 (2012).

62. Miettinen, T. P. & Björklund, M. Mitochondrial Function and Cell Size: An Allometric Relationship. *Trends Cell Biol.* **27,** 393–402 (2017).

63. Pollak, J. K. & Munn, E. A. The isolation by isopycnic density-gradient centrifugation of two mitochondrial populations from livers of embryonic and fed and starved adult rats. *Biochem. J.* **117,** 913–919 (1970).

64. Bryan, A. K., Goranov, A., Amon, A. & Manalis, S. R. Measurement of mass, density, and volume during the cell cycle of yeast. *Proc. Natl. Acad. Sci. U. S. A.* **107,** 999–1004 (2010).

65. Balakrishnan, R., Park, J., Karra, K., *et al.* YeastMine-An integrated data warehouse for Saccharomyces cerevisiae data as a multipurpose tool-kit. *Database* **2012,** bar062 (2012).

66. Vogel, F., Bornhövd, C., Neupert, W. & Reichert, A. S. Dynamic subcompartmentalization of the mitochondrial inner membrane. *J. Cell Biol.* **175,** 237–247 (2006).

67. Pfanner, N., van der Laan, M., Amati, P., *et al.* Uniform nomenclature for the mitochondrial contact site and cristae organizing system. *J. Cell Biol.* **204,** 1083–1086 (2014).

68. Cogliati, S., Frezza, C., Soriano, M. E., *et al.* Mitochondrial cristae shape determines respiratory chain supercomplexes assembly and respiratory efficiency. *Cell* **155,** 160–171 (2013).

69. Rampelt, H., Zerbes, R. M., van der Laan, M. & Pfanner, N. Role of the mitochondrial contact site and cristae organizing system in membrane architecture and dynamics. *Biochim. Biophys. Acta* **1864,** 737–746 (2017).

70. Meeusen, S., DeVay, R., Block, J., *et al.* Mitochondrial Inner-Membrane Fusion and Crista Maintenance Requires the Dynamin-Related GTPase Mgm1. *Cell* **127,** 383–395 (2006).

71. Budin, I., de Rond, T., Chen, Y., *et al.* Viscous control of cellular respiration by membrane lipid composition. *Science* **362,** 1186–1189 (2018).

72. Gu, Z., Valianpour, F., Chen, S., *et al.* Aberrant cardiolipin metabolism in the yeast taz1 mutant: A model for Barth syndrome. *Mol. Microbiol.* **51,** 149–158 (2004).

73. Beranek, A., Rechberger, G., Knauer, H., *et al.* Identification of a cardiolipin-specific phospholipase encoded by the gene CLD1 (YGR110W) in yeast. *J. Biol. Chem.* **284,** 11572–11578 (2009).

74. Pfanner, N., Warscheid, B. & Wiedemann, N. Mitochondrial proteins: from biogenesis to functional networks. *Nat. Rev. Mol. Cell Biol.* **20,** 267–284 (2019).

75. Nunnari, J. & Suomalainen, A. Mitochondria: In sickness and in health. *Cell* **148,** 1145–1159 (2012).

76. Smith, A. C. & Robinson, A. J. MitoMiner v4.0: an updated database of mitochondrial localization evidence , phenotypes and diseases. *Nucleic Acids Res.* **47,** D1225–D1228 (2019).

77. Saha, R., Chowdhury, A. & Maranas, C. D. Recent advances in the reconstruction of metabolic models and integration of omics data. *Curr. Opin. Biotechnol.* **29,** 39–45 (2014).

78. O'Brien, E. J., Monk, J. M. & Palsson, B. O. Using genome-scale models to predict biological capabilities. *Cell* **161,** 971–987 (2015).

79. Vo, T. D., Greenberg, H. J. & Palsson, B. O. Reconstruction and functional characterization of the human mitochondrial metabolic network based on proteomic and biochemical data. *J. Biol. Chem.* **279,** 39532–39540 (2004).

80. Thiele, I., Price, N. D., Vo, T. D. & Palsson, B. O. Candidate metabolic network states in human mitochondria. *J. Biol. Chem.* **280,** 11683–11695 (2005).

81. Smith, A. C. & Robinson, A. J. A metabolic model of the mitochondrion and its use in modelling diseases of the tricarboxylic acid cycle. *BMC Syst. Biol.* **5,** 102 (2011).

82. Zieliński, Ł. P., Smith, A. C., Smith, A. G. & Robinson, A. J. Metabolic flexibility of mitochondrial respiratory chain disorders predicted by computer modelling. *Mitochondrion* **31,** 45–55 (2016).

83. Smith, A. C., Eyassu, F., Mazat, J. P. & Robinson, A. J. MitoCore: a curated constraint-based model for simulating human central metabolism. *BMC Syst. Biol.* **11,** 114 (2017).

84. Lu, H., Li, F., Sánchez, B. J., *et al.* A consensus S. cerevisiae metabolic model Yeast8 and its ecosystem for comprehensively probing cellular metabolism. *Nat. Commun.* **10,** 3586 (2019).

85. Domenzain, I., Sánchez, B., Anton, M., *et al.* Reconstruction of a catalogue of genome-scale metabolic models with enzymatic constraints using GECKO 2.0. *bioRxiv.* https://doi.org/10.1101/2021.03.05.433259 (2021).

86. Mitchell, P. Coupling of Phosphorylation to Electron and Hydrogen Transfer by a Chemi-Osmotic type of Mechanism. *Nature* **191,** 144–148 (1961).

87. Beauvoit, B., Rigoulet, M. & Guerin, B. Thermodynamic and kinetic control of ATP synthesis in yeast mitochondria: role of delta pH. *FEBS Lett.* **244,** 255–8 (1989).

88. Verduyn, C., Stouthamer, A. H., Scheffers, W. A. & van Dijken, J. P. A theoretical evaluation of growth yields of yeasts. *Antonie Van Leeuwenhoek* **59,** 49–63 (1991).

89. Van Hoek, P., Van Dijken, J. P. & Pronk, J. T. Effect of specific growth rate on fermentative capacity of baker's yeast. *Appl. Environ. Microbiol.* **64,** 4226–4233 (1998).

90. Wiedemann, N. & Pfanner, N. Mitochondrial Machineries for Protein Import and Assembly. *Annu. Rev. Biochem.* **86,** 685–714 (2017).

91. Chacinska, A., Pfannschmidt, S., Wiedemann, N., *et al.* Essential role of Mia40 in import and assembly of mitochondrial intermembrane space proteins. *EMBO J.* **23,** 3735–3746 (2004).

92. Wiedemann, N., Kozjak, V., Chacinska, A., *et al.* Machinery for protein sorting and assembly in the mitochondrial outer membrane. *Nature* **424,** 565–571 (2003).

93. Becker, T., Pfannschmidt, S., Guiard, B., *et al.* Biogenesis of the mitochondrial TOM complex: Mim1 promotes insertion and assembly of signal-anchored receptors. *J. Biol. Chem.* **283,** 120–127 (2008).

94. Schulz, C., Schendzielorz, A. & Rehling, P. Unlocking the presequence import pathway. *Trends Cell Biol.* **25,** 265–275 (2015).

95. Botelho, S. C., Österberg, M., Reichert, A. S., *et al.* TIM23-mediated insertion of transmembrane α-helices into the mitochondrial inner membrane. *EMBO J.* **30,** 1003–1011 (2011).

96. Stiller, S. B., Höpker, J., Oeljeklaus, S., *et al.* Mitochondrial OXA Translocase Plays a Major Role in Biogenesis of Inner-Membrane Proteins. *Cell Metab.* **23,** 901–908 (2016).

97. Sirrenberg, C., Bauer, M. F., Guiard, B., Neupert, W. & Brunner, M. Import of carrier proteins into the mitochondrial inner membrane mediated by Tim22. *Nature* **384,** 582–585 (1996).

98. Lahtvee, P.-J., Sánchez, B. J., Smialowska, A., *et al.* Absolute Quantification of Protein and mRNA Abundances Demonstrate Variability in Gene-Specific Translation Efficiency in Yeast. *Cell Syst.* **4,** 495–504 (2017).

99. Rudiger, S., Buchberger, A. & Bukau, B. Interaction of Hsp70 chaperones with substrates. *Nat. Struct. Biol.* **4,** 342–349 (1997).

100. Ho, B., Baryshnikova, A. & Brown, G. W. Unification of Protein Abundance Datasets Yields a Quantitative Saccharomyces cerevisiae Proteome. *Cell Syst.* **6,** 192–205 (2018).

101. Jeske, L., Placzek, S., Schomburg, I., Chang, A. & Schomburg, D. BRENDA in 2019: a European ELIXIR core data resource. *Nucleic Acids Res.* **47,** D542–D549 (2019).

102. The UniProt Consortium. UniProt: a worldwide hub of protein knowledge. *Nucleic Acids Res.* **47,** D506–D515 (2019).

103. Scott, M., Gunderson, C. W., Mateescu, E. M., Zhang, Z. & Hwa, T. Interdependence of Cell Growth and Gene Expression: Origins and Consequences. *Science* **330,** 1099–1102 (2010).

104. You, C., Okano, H., Hui, S., *et al.* Coordination of bacterial proteome with metabolism by cyclic AMP signalling. *Nature* **500,** 301–306 (2013).

105. Hui, S., Silverman, J. M., Chen, S. S., *et al.* Quantitative proteomic analysis reveals a simple strategy of global resource allocation in bacteria. *Mol. Syst. Biol.* **11,** 784 (2015).

106. Basan, M., Hui, S., Okano, H., *et al.* Overflow metabolism in Escherichia coli results from efficient proteome allocation. *Nature* **9,** 99–106 (2015).

107. Huang, M., Bai, Y., Sjostrom, S. L., *et al.* Microfluidic screening and whole-genome sequencing identifies mutations associated with improved protein secretion by yeast. *Proc. Natl. Acad. Sci. U. S. A.* **112,** E4689–E4696 (2015).

108. Dubois, E., Hiernaux, D., Grenson, M. & Wiame, J. M. Specific induction of catabolism and its relation to repression of biosynthesis in arginine metabolism of Saccharomyces cerevisiae. *J. Mol. Biol.* **122,** 383–406 (1978).

109. Yoon, S., Govind, C. K., Qiu, H., *et al.* Recruitment of the ArgR/Mcm1p repressor is stimulated by the activator Gcn4p: A self-checking activation mechanism. *Proc. Natl. Acad. Sci. U. S. A.* **101,** 11713–11718 (2004).

110. Monschau, N., Stahmann, K. P., Sahm, H., McNeil, J. B. & Bognar, A. L. Identification of Saccharomyces cerevisiae GLY1 as a threonine aldolase: a key enzyme in glycine biosynthesis. *FEMS Microbiol. Lett.* **150,** 55–60 (1997).

111. Thomas, D. & Surdin-Kerjan, Y. Metabolism of sulfur amino acids in Saccharomyces cerevisiae. *Microbiol. Mol. Biol. Rev.* **61,** 503–532 (1997).

112. Yu, R., Vorontsov, E., Sihlbom, C. & Nielsen, J. Quantifying absolute gene expression profiles reveals distinct regulation of central carbon metabolism genes in yeast. *eLife* **10,** e65722 (2021).

113. Gangloff, S. P., Marguet, D. & Lauquin, G. J. Molecular cloning of the yeast mitochondrial aconitase gene (ACO1) and evidence of a synergistic regulation of expression by glucose plus glutamate. *Mol. Cell. Biol.* **10,** 3551–3561 (1990).

114. Camarasa, C., Grivet, J. P. & Dequin, S. Investigation by 13C-NMR and tricarboxylic acid (TCA) deletion mutant analysis of pathways of succinate formation in Saccharomyces cerevisiae during anaerobic fermentation. *Microbiology* **149,** 2669–2678 (2003).

115. Fazius, F., Shelest, E., Gebhardt, P. & Brock, M. The fungal α-aminoadipate pathway for lysine biosynthesis requires two enzymes of the aconitase family for the isomerization of homocitrate to homoisocitrate. *Mol. Microbiol.* **86,** 1508–1530 (2012).

116. Nilsson, A. & Nielsen, J. Metabolic Trade-offs in Yeast are Caused by F1F0-ATP synthase. *Sci. Rep.* **6,** 22264 (2016).

117. Chen, Y. & Nielsen, J. Energy metabolism controls phenotypes by protein efficiency and allocation. *Proc. Natl. Acad. Sci. U. S. A.* **116,** 17592–17597 (2019).

118. Fonseca, G. G., Barbosa de Carvalho, N. M. & Gombert, A. K. Growth of the yeast Kluyveromyces marxianus CBS 6556 on different sugar combinations as sole carbon and energy source. *Appl. Microb. Cell Physiol.,* 5055–5067 (2013).

119. Fonseca, G. G., Gombert, A. K., Heinzle, E. & Wittmann, C. Physiology of the yeast Kluyveromyces marxianus during batch and chemostat cultures with glucose as the sole carbon source. *FEMS Yeast Res.* **7,** 422–435 (2007).

120. Shi, N. Q., Cruz, J., Sherman, F. & Jeffries, T. W. SHAM-sensitive alternative respiration in the xylose-metabolizing yeast Pichia stipitis. *Yeast* **19,** 1203–1220 (2002).

121. Thompson, A., Schäfer, J., Kuhn, K., *et al.* Tandem mass tags: A novel quantification strategy for comparative analysis of complex protein mixtures by MS/MS. *Anal. Chem.* **75,** 1895–1904 (2003).

122. Domenzain, I., Li, F., Kerkhoven, E. J. & Siewers, V. Evaluating accessibility, usability and interoperability of genome-scale metabolic models for diverse yeasts species. *FEMS Yeast Res.* **21,** foab002 (2021).

123. Fiaux, J., Çakar, Z. P., Sonderegger, M., *et al.* Metabolic-Flux Profiling of the Yeasts Saccharomyces cerevisiae and Pichia stipitis. *Eukaryot. Cell* **2,** 170–180 (2003).

124. Blank, L. M., Lehmbeck, F. & Sauer, U. Metabolic-flux and network analysis in fourteen hemiascomycetous yeasts. *FEMS Yeast Res.* **5,** 545–558 (2005).

125. Papini, M., Nookaew, I., Uhlén, M. & Nielsen, J. Scheffersomyces stipitis: A comparative systems biology study with the Crabtree positive yeast Saccharomyces cerevisiae. *Microb. Cell Fact.* **11,** 1–16 (2012).

126. Pronk, J. T., Steensma, H. Y. & Van Dijken, J. P. Pyruvate metabolism in Saccharomyces cerevisiae. *Yeast* **12,** 1607–1633 (1996).

127. Consortium, T. G. O. The Gene Ontology Resource: 20 years and still GOing strong. *Nucleic Acids Res.* **47,** D330–D338 (2019).

128. Wolfe, K. H. & Shields, D. C. Molecular evidence for an ancient duplication of the entire yeast genome. *Nature* **387,** 708–13 (1997).

129. Conant, G. C. & Wolfe, K. H. Increased glycolytic flux as an outcome of whole-genome duplication in yeast. *Mol. Syst. Biol.* **3,** 129 (2007).

130. Rhind, N., Chen, Z., Yassour, M., *et al.* Comparative functional genomics of the fission yeasts. *Science* **332,** 930–936 (2011).

131. Elbing, K., Larsson, C., Bill, R. M., *et al.* Role of hexose transport in control of glycolytic flux in Saccharomyces cerevisiae. *Appl. Environ. Microbiol.* **70,** 5323–5330 (2004).

132. Lin, Z. & Li, W. H. Expansion of hexose transporter genes was associated with the evolution of aerobic fermentation in yeasts. *Mol. Biol. Evol.* **28,** 131–142 (2011).

133. Vemuri, G. N., Eiteman, M. A., McEwen, J. E., Olsson, L. & Nielsen, J. Increasing NADH oxidation reduces overflow metabolism in Saccharomyces cerevisiae. *Proc. Natl. Acad. Sci. U. S. A.* **104,** 2402–2407 (2007).

134. Seoighe, C. & Wolfe, K. H. Yeast genome evolution in the post-genome era. *Curr. Opin. Microbiol.* **2,** 548–554 (1999).

135. Sickmann, A., Reinders, J., Wagner, Y., *et al.* The proteome of Saccharomyces cerevisiae mitochondria. *Proc. Natl. Acad. Sci. U. S. A.* **100,** 13207–12 (2003).

136. Reinders, J., Zahedi, R. P., Pfanner, N., *et al.* Toward the Complete Yeast Mitochondrial Proteome : Multidimensional Separation Techniques for Mitochondrial Proteomics. *J. Proteome Res.* **5,** 1543–1554 (2006).

137. Nilsson, A., Nielsen, J. & Palsson, B. O. Metabolic Models of Protein Allocation Call for the Kinetome. *Cell Syst.* **5,** 538–541 (2017).

138. Davidi, D., Noor, E., Liebermeister, W., *et al.* Global characterization of in vivo enzyme catalytic rates and their correspondence to in vitro k cat measurements. *Proc. Natl. Acad. Sci. U. S. A.* **113,** 3401–3406 (2016).

139. Liu, J. K., O'brien, E. J., Lerman, J. A., *et al.* Reconstruction and modeling protein translocation and compartmentalization in Escherichia coli at the genome-scale. *BMC Syst. Biol.* **8** (2014).

140. Oftadeh, O., Salvy, P., Masid, M., *et al.* A genome-scale metabolic model of Saccharomyces cerevisiae that integrates expression constraints and reaction thermodynamics. *bioRxiv.* https://doi.org/10.1101/2021.02.17.431671 (2021).

141. Elsemman, I. E., Rodrigues Prado, A., Grigaitis, P., *et al.* Whole-cell modeling in yeast predicts compartment-specific proteome constraints that drive metabolic strategies. *bioRxiv.* https://doi.org/10.1101/2021.06.11.448029 (2021).

142. Robinson, J. L., Kocabaş, P., Wang, H., *et al.* An atlas of human metabolism. *Sci. Signal.* **13,** 1–12 (2020).

143. Yu, R., Campbell, K., Pereira, R., *et al.* Nitrogen limitation reveals large reserves in metabolic and translational capacities of yeast. *Nat. Commun.* **11,** 1181 (2020).

144. Klumpp, S., Scott, M., Pedersen, S. & Hwa, T. Molecular crowding limits translation and cell growth. *Proc. Natl. Acad. Sci. U. S. A.* **110,** 16754–16759 (2013).

145. Kafri, M., Metzl-Raz, E., Jona, G. & Barkai, N. The Cost of Protein Production. *Cell Rep.* **14,** 22–31 (2016).

146. D'Souza, G., Waschina, S., Pande, S., *et al.* Less is more: Selective advantages can explain the prevalent loss of biosynthetic genes in bacteria. *Evolution* **68,** 2559–2570 (2014).

147. Yang, L., Yurkovich, J. T., Lloyd, C. J., *et al.* Principles of proteome allocation are revealed using proteomic data and genome-scale models. *Sci. Rep.* **6,** 6–13 (2016).

148. Dill, K. A., Ghosh, K. & Schmit, J. D. Physical limits of cells and proteomes. *Proc. Natl. Acad. Sci. U. S. A.* **108,** 17876–17882 (2011).

149. Kostinski, S. & Reuveni, S. Ribosome Composition Maximizes Cellular Growth Rates in E. coli. *Phys. Rev. Lett.* **125,** 28103 (2020).

150. Belliveau, N. M., Chure, G., Hueschen, C. L., *et al.* Fundamental limits on the rate of bacterial growth and their influence on proteomic composition. *Cell Syst.* **12,** 1–21 (2021).

151. Valgepea, K., Peebo, K., Adamberg, K., Vilu, R. & Dien, S. V. Lean-proteome strains – next step in metabolic engineering. *Front Bioeng Biotechnol.* **3,** 11 (2015).